Naval Surface Warfare Center
Carderock Division
West Bethesda, MD 20817-5700

NSWCCD-TR-2000/011 July 2000

Hydrodynamics Directorate

Technical Report

Analytical Representation of Ship Waves

(23rd Weinblum Memorial Lecture)

by

Francis Noblesse

NSWCCD-TR–2000/011 Analytical Representation of Ship Waves (23rd Weinblum Memorial Lecture)

REPORT DOCUMENTATION PAGE

Form Approved
OMB No. 0704-0188

1. AGENCY USE ONLY *(Leave blank)*	2. REPORT DATE	3. REPORT TYPE AND DATES COVERED
	1 July 2000	R&D Final

4. TITLE AND SUBTITLE
Analytical Representation of Ship Waves
(23rd Weinblum Memorial Lecture)

5. FUNDING NUMBERS
Program Element 0601152N
Work Request WX20295
Task Area ZR-000-01-01
Work Unit 1-5200-069

6. AUTHOR(S)
Francis Noblesse

7. PERFORMING ORGANIZATION NAME(S) AND ADDRESS(ES)
NAVAL SURFACE WARFARE CENTER
CARDEROCK DIVISION (CODE 5500)
9500 MACARTHUR BOULEVARD
WEST BETHESDA, MD 20817-5700

8. PERFORMING ORGANIZATION REPORT NUMBER
NSWCCD-TR–2000/011

9. SPONSORING/MONITORING AGENCY NAME(S) AND ADDRESS(ES)
INDEPENDENT LABORATORY INDEPENDENT RESEARCH (ILIR) PROGRAM
NAVAL SURFACE WARFARE CENTER
CARDEROCK DIVISION (CODE 0112)
9500 MACARTHUR BOULEVARD
WEST BETHESDA, MD 20817-5700

10. SPONSORING/MONITORING AGENCY REPORT NUMBER

11. SUPPLEMENTARY NOTES

12a. DISTRIBUTION/AVAILABILITY STATEMENT
Approved for public release; distribution is unlimited.

12b. DISTRIBUTION CODE

13. ABSTRACT ***(Maximum 200 words)***

Four fundamental analytical representations of time-harmonic ship waves, and the particular cases of steady ship waves and wave diffraction-radiation without forward speed, are summarized. These analytical representations are (i) a boundary-integral representation, called velocity representation, that defines a free-surface potential flow in terms of a velocity distribution at a boundary surface, (ii) a practical Fourier representation of super Green functions associated with a broad class of dispersive waves and arbitrary singularity distributions, (iii) a simple representation, called Fourier-Kochin wave representation, of the waves due to an arbitrary boundary velocity distribution, (iv) a corresponding representation of local flows, called Rankine and Fourier-Kochin representation, based on the velocity representation, the Fourier-Kochin approach, and a Rankine-Fourier decomposition process. The four analytical representations are the main results underlying the Fourier-Kochin theory of ship waves. The results are organized in an order intended to provide a coherent and complete overview of this theory.

14. SUBJECT TERMS
wave diffraction-radiation
ship waves
ship motions
Fourier-Kochin theory

15. NUMBER OF PAGES
48

16. PRICE CODE

17. SECURITY CLASSIFICATION OF REPORT	18. SECURITY CLASSIFICATION OF THIS PAGE	19. SECURITY CLASSIFICATION OF ABSTRACT	20. LIMITATION OF ABSTRACT
UNCLASSIFIED	UNCLASSIFIED	UNCLASSIFIED	SAR

NSN 7540-01-280-5500

Standard Form 298 (Rev. 2-89)
Prescribed by ANSI Std. Z39-18
298-102

CONTENTS

ADMINISTRATIVE INFORMATION

This study was performed with support from the Independent Laboratory Independent Research (ILIR) Program at the Carderock Division, Naval Surface Warfare Center, West Bethesda, MD. Program Element 0601152N; Work Request WX20295; Task Area ZR-000-01-01; Work Unit 1-5200-069.

ACKNOWLEDGMENTS

This summary of the Fourier-Kochin theory would be incomplete without the acknowledgment of my debt to Dr. Chi Yang (George Mason University) and Dr. Xiao-Bo Chen (Bureau Veritas) for their work related to the Fourier representation of generic super Green functions. I am also much indebted to Dr. Dane Hendrix (David Taylor Model Basin), Dr. Chi Yang and Prof. Rainald Lohner (George Mason University) for their critical work on practical applications of the theory and to my wife Annie Tabarie for numerous "Fourier-Kochin week-ends" over the past decade. Finally the support of the Independent Laboratory Independent Research (ILIR) research program at the David Taylor Model Basin has been of utmost importance and is deeply appreciated.

Introduction

This study mostly considers three basic classes of free-surface flows related to interactions of water waves with floating bodies like ships and offshore structures : (i) time-harmonic flow associated with diffraction-radiation of regular waves by a floating body without forward speed, e.g. an offshore structure, (ii) steady flow due to a ship advancing in calm water, (iii) time-harmonic flow due to a ship advancing in regular waves, i.e. wave diffraction-radiation with forward speed. The body of water is assumed to be of infinite depth and lateral extent.

The classical potential-flow theoretical framework is adopted. This framework correctly represents the aspects of ship wavemaking and wave diffraction-radiation by ships and offshore structures that are of primary practical significance (notably forces, pressure distributions, and wave patterns). Furthermore, potential-flow theory is the only framework that provides practical means of analyzing steady ship waves and wave diffraction-radiation in various wave environments for routine applications, and for hull-form optimization (ultimately required for superior designs).

Mathematics has been used extensively to analyze free-surface flows (and more generally fluid flows) in various special cases, including special geometries (e.g. 2D flows, and 3D flows about simple bodies like spheres and spheroids) and limiting cases associated with a perturbation analysis (e.g. thin-ship and slender-body theories, and theories based on low or high ship-speed or wave-frequency approximations). This traditional role of mathematics, which may be named "mathematics for special cases", has provided a wealth of useful results. Another important role of mathematics, which may be named "mathematics for the computer age", consists in developing mathematical formulations that make it possible to perform robust, accurate, and efficient numerical calculations, without restriction with regard to hull form, ship speed, and wave frequency. Mathematics is used here for the latter purpose.

Specifically, four fundamental analytical representations of the three classes of free-surface flows under consideration are summarized. These analytical representations are the main results that underly the Fourier-Kochin theory of ship waves. The four analytical representations are presented in an order and a manner intended to provide a coherent and complete overview of this theory.

Two complementary elementary solutions of Laplace's equation

An important fundamental solution of the Laplace equation is the elementary wave function

$$\exp[\sqrt{\alpha^2+\beta^2}\,\zeta - i\,(\alpha\,\xi+\beta\,\eta)\,] \tag{1a}$$

Here, α and β are real. Another important class of fundamental solutions of Laplace's equation is the elementary Rankine singularity $1/r$ and the related Rankine sources $1/r'$ and $1/r''$ with r, r', r'' given by

$$\left\{\begin{array}{l} r = \sqrt{(\xi-x)^2+(\eta-y)^2+(\zeta-z)^2} \\ r' = \sqrt{(\xi-x)^2+(\eta-y)^2+(\zeta+z)^2} \\ r'' = \sqrt{(\xi-x)^2+(\eta-y)^2+(\zeta+z-C^2)^2} \end{array}\right\} \tag{1b}$$

Here, C^2 is a positive real constant.

The elementary wave (1a) and the elementary Rankine singularity $1/r$ are related via the Fourier transformation (see Appendix 1)

$$\frac{1}{r} = \frac{1}{2\,\pi}\int_{-\infty}^{\infty} d\beta \int_{-\infty}^{\infty} d\alpha\, \frac{\mathcal{E}}{k}\, e^{-k\,|\zeta-z|} \tag{2a}$$

with

$$k = \sqrt{\alpha^2+\beta^2} \qquad \mathcal{E} = e^{-i\,[\alpha\,(\xi-x)+\beta\,(\eta-y)]} \tag{2b}$$

Expression (2a) shows that, for $\zeta + z \leq 0$, the related Rankine sources $1/r'$ and $1/r''$ can similarly be expressed as

$$\frac{1}{r'} = \frac{1}{2\,\pi}\int_{-\infty}^{\infty} d\beta \int_{-\infty}^{\infty} d\alpha\, \frac{\mathcal{E}}{k}\, e^{k\,(\zeta+z)} \tag{2c}$$

$$\frac{1}{r''} = \frac{1}{2\,\pi}\int_{-\infty}^{\infty} d\beta \int_{-\infty}^{\infty} d\alpha\, \frac{\mathcal{E}}{k}\, e^{k\,(\zeta+z-C^2)} \tag{2d}$$

The Fourier relations (2) indicate that free-surface flows can in principle be represented using exclusively Rankine singularities or elementary waves. However, these two "extreme" approaches are not the most appropriate because Rankine singularities and elementary waves are complementary elementary solutions of the Laplace equation that are ideally suited for representing nonoscillatory local flow disturbances and waves, respectively.

Free-surface boundary conditions

Consider a ship advancing in waves along a straight path, with constant speed $\mathcal{U}$. The X axis is chosen along the path of the ship, and points toward the ship bow. Thus, the ship advances in the direction of the positive X axis. The Z axis is vertical and points upward, and the mean free surface is taken as the plane $Z=0$. The flow is observed from a Cartesian system of coordinates moving with speed $\mathcal{U}$ along the X axis, and is expressed as the sum of a steady-flow component, which represents the flow due to the ship advancing in calm water, and an unsteady-flow component associated with the ambient waves, the waves diffracted by the ship, and the radiated waves due to the motions of the ship about a mean position.

Within the framework of a linear potential-flow analysis, the velocity potential Φ associated with the unsteady flow due to the ship satisfies the free-surface boundary condition

$$g\,\Phi_Z + (\,\partial_T - \mathcal{U}\,\partial_X\,)^2\,\Phi = 0 \quad \text{at} \quad Z = 0$$

where T stands for time and g is the gravitational acceleration. A frequency-domain analysis is considered. Thus, the time-harmonic flow due to a ship advancing through an elementary wave is now examined. The velocity potential of a linear time-harmonic flow can be defined as the limit, when the growth parameter $\mu \to +0$, of the flow given by the potential

$$\Re e\ \Phi(\vec{X})\ \exp(\,\mu T/2 - i\,\omega T\,)$$

where $\Re e$ stands for the real part and ω is the frequency of the waves encountered by the advancing ship. This expression for the potential is associated with a flow that may be imagined to start at the time $T = -\infty$ from a state of rest (since $\mu > 0$), corresponding to the initial conditions $\Phi = 0$ and $\Phi_T = 0$. The free-surface boundary condition becomes

$$g\,\Phi_Z - (\,\omega + i\,\mu/2 - i\,\mathcal{U}\,\partial_X\,)^2\,\Phi = 0$$

The time-harmonic flow due to the ship can be formulated in nondimensional form in terms of the water density, a reference length L and a reference velocity U. E.g., L and U may respectively be taken as the length and the speed $\mathcal{U}$ of the ship. The free-surface condition associated with the nondimensional coordinates $\vec{\xi} = \vec{X}/L$ and potential $\phi = \Phi/(UL)$ is

$$\phi_\zeta - (\,f + i\,\varepsilon/2 - i\,F\,\partial_\xi\,)^2\,\phi = 0$$

with

$$f = \omega\sqrt{L/g} \qquad \varepsilon = \mu\sqrt{L/g} \qquad F = \mathcal{U}/\sqrt{gL}$$

For $0 < \varepsilon \ll 1$, the free-surface condition becomes

$$\phi_\zeta - (f - iF\partial_\xi)^2\phi - i\varepsilon(f - iF\partial_\xi)\phi = 0$$

Thus, the linearized free-surface boundary condition associated with diffraction-radiation of time-harmonic waves with forward speed is

$$\phi_\zeta - f^2\phi + i2\tau\phi_\xi + F^2\phi_{\xi\xi} - \varepsilon(if\phi + F\phi_\xi) = p \tag{3a}$$

where $\tau = fF$ is the Brard number, and p stands for a nonhomogeneous forcing term. E.g., p may account for a pressure distribution at the free surface. The linear free-surface condition associated with steady ship waves can similarly be shown to be

$$\phi_\zeta + F^2\phi_{\xi\xi} - \varepsilon F\phi_\xi = p \tag{3b}$$

Here, $\nabla\phi$ stands for the disturbance velocity due to the ship. Finally, the free-surface condition for linear time-harmonic flows without forward speed is

$$\phi_\zeta - f^2\phi - i\varepsilon f\phi = p \tag{3c}$$

The free-surface conditions (3b) and (3c) evidently correspond to the special cases $f=0$ and $F=0$ of the ship-motion condition (3a).

Dispersion functions and dispersion curves

The elementary wave solution (1a) of the Laplace equation satisfies the homogeneous free-surface boundary conditions (3) if the Fourier variables α and β satisfy the relation $D_\varepsilon = 0$, where the function $D_\varepsilon = 0$ is defined as

$$D_\varepsilon = D + i\varepsilon D' \tag{4a}$$

with D and D' given by

$$D = \begin{Bmatrix} (f-F\alpha)^2 - k \\ F^2\alpha^2 - k \\ f^2 - k \end{Bmatrix} \quad D' = \begin{Bmatrix} f-F\alpha \\ -F\alpha \\ f \end{Bmatrix} \quad \text{if} \begin{Bmatrix} fF > 0 \\ f = 0 \\ F = 0 \end{Bmatrix} \tag{4b}$$

In expressions (4b) for the function D, called dispersion function, $k = \sqrt{\alpha^2+\beta^2}$ is the wavenumber. Farfield waves corresponding to the free-surface boundary conditions (3) are given by one-dimensional Fourier superpositions of elementary waves (1a) since the Fourier variables α and β

are related by the dispersion relation $D=0$. In fact, the dispersion relation $D=0$ typically defines several curves (although a single curve may be defined in some simple cases) in the Fourier plane (α, β). These curves, called dispersion curves, have an important role in the Fourier representation of farfield and nearfield waves. The dispersion curves associated with the dispersion relations (4b) are now considered.

For time-harmonic flows without forward speed, the dispersion relation $D=0$ defines the single closed dispersion curve

$$k = f^2 \tag{5a}$$

which evidently is a circle centered at the origin $k = 0$ of the Fourier plane. For steady flows, the dispersion relation $k = F^2\alpha^2$ defines two open dispersion curves given by

$$\beta = \pm|\,\alpha\,|\,\sqrt{F^4\alpha^2 - 1} \tag{5b}$$

with $F^2|\alpha| \geq 1$. These dispersion curves are symmetric about both $\beta = 0$ and $\alpha = 0$. The ship-motion dispersion relation $D=0$ corresponding to the case $\tau = fF > 0$ yields

$$\beta = \pm\sqrt{(f - F\alpha)^4 - \alpha^2} \tag{5c}$$

The dispersion curves defined by (5c) are symmetric with respect to $\beta = 0$. The ship-motion dispersion relation (5c) defines two or three dispersion curves if τ is larger or smaller than $1/4$.

If $\tau < 1/4$, the three dispersion curves intersect the axis $\beta = 0$ at four values of α, which are denoted $\alpha_i^{\pm}$ and $\alpha_o^{\pm}$ and are given by

$$\left\{ \begin{array}{l} \pm\alpha_i^{\pm} = f^2\,(\sqrt{1/4 \pm \tau} - 1/2)^2/\tau^2 \\ \pm\alpha_o^{\pm} = (\sqrt{1/4 \pm \tau} + 1/2)^2/F^2 \end{array} \right\} \tag{6}$$

The three dispersion curves are found in the regions

$$\alpha \leq \alpha_o^- \qquad \alpha_i^- \leq \alpha \leq \alpha_i^+ \qquad \alpha_o^+ \leq \alpha \tag{7a}$$

If $\tau = 1/4$, (6) yield

$$\alpha_o^- = \alpha_i^- = -f/F = -\omega\, L/\mathcal{U}$$

and the dispersion curves in the regions $\alpha \leq \alpha_o^-$ and $\alpha_i^- \leq \alpha \leq \alpha_i^+$ are connected. If $\tau > 1/4$, the roots α_o^- and α_i^- are complex and we only have two dispersion curves, located in the regions

$$\alpha \leq \alpha_i^+ \qquad \alpha_o^+ \leq \alpha \tag{7b}$$

The inner roots $\alpha_i^{\pm}$ and the outer roots $\alpha_o^{\pm}$ satisfy the inequalities

$$\left\{\begin{array}{c} \alpha_o^- < -f/F < \alpha_i^- < 0 < \alpha_i^+ < f/F < \alpha_o^+ \\ \alpha_i^+ < |\alpha_i^-| < |\alpha_o^-| < \alpha_o^+ \end{array}\right\} \tag{8}$$

The dispersion curves defined by (5), (6) and (7) are depicted for $\tau = 0.2, 0.25, 0.3$ in Fig. 1, where the Fourier plane is scaled with respect to f/F.

In the limit $\tau = 0$, (6) yield $\alpha_i^{\pm} = \pm f^2$ and $\alpha_o^{\pm} = \pm 1/F^2$. More generally, we have

$$\alpha_i^{\pm} \approx \pm f^2 \qquad \alpha_o^{\pm} \approx \pm 1/F^2 \qquad \text{for } \tau \ll 1$$

Thus, the dispersion curves in the outer regions $\alpha \leq \alpha_o^-$ and $\alpha_o^+ \leq \alpha$ correspond to values of the wavenumber k that are greater than $1/F^2$ (approximately), whereas we have $k \approx f^2$ for the dispersion curve in the inner region $\alpha_i^- \leq \alpha \leq \alpha_i^+$. The ratio of the wavenumbers k_i and k_o associated with the inner and outer dispersion curves, given by $k_i/k_o \approx \tau^2$, is very small if τ is small, say if $\tau \leq 0.2$. Thus, scaling of the Fourier coordinates α and β with respect to f^2 and $1/F^2$ is proper in this regime. The upper and lower parts of Fig. 2 respectively depict the inner and outer dispersion curves for several values of τ in the frequency-scaled and speed-scaled Fourier planes $(\alpha, \beta)/f^2$ and $F^2(\alpha, \beta)$. Finally, (6) yield

$$\alpha_i^+ \sim f/F \sim \alpha_o^+ \quad \text{as } \tau \to \infty$$

Thus, scaling of the Fourier coordinates with respect to f/F is proper for large values of τ.

Free-surface Green functions

The Green function $G(\vec{\xi}, \vec{x})$ associated with the ship-motion free-surface boundary condition (3a) satisfies the free-surface boundary condition

$$G_\zeta - f^2 G + i\, 2\tau\, G_\xi + F^2 G_{\xi\xi} - \varepsilon\,(ifG + FG_\xi) = 0 \tag{9}$$

at $\zeta = 0$. $G(\vec{\xi}, \vec{x})$ is the velocity potential of the flow created at the field point $\vec{\xi} = (\xi, \eta, \zeta \leq 0)$ by a pulsating source located at the singular point $\vec{x} = (x, y, z \leq 0)$. Green functions associated with a boundary condition like (9), which holds at the plane $\zeta = 0$, can be expressed as

$$G(\vec{\xi}, \vec{x}) = G^S(\xi - x, \eta - y, \zeta - z) + G^F(\xi - x, \eta - y, \zeta + z) \tag{10a}$$

where G^S corresponds to a simple Rankine source and G^F accounts for free-surface effects. The Rankine component G^S is defined by

$$4\pi\, G^S = -1/r \tag{10b}$$

with r given by (1b). The free-surface component G^F in expression (10a) corresponding to the free-surface condition (9) is given by (see Appendix 2)

$$4\pi G^F = \lim_{\varepsilon \to +0} \frac{1}{\pi} \int_{-\infty}^{\infty} d\beta \int_{-\infty}^{\infty} d\alpha \, \frac{A^F}{D_\varepsilon} \, e^{k(\zeta + z)} \mathcal{E} \tag{11a}$$

Here, k and $\mathcal{E}$ are given by (2b), D_ε is the dispersion function defined by (4), and the amplitude function A^F is given by

$$A^F = [(f - F\alpha)^2 + k]/(2k) \tag{11b}$$

The free-surface component G^F in (10a) is usually expressed in the alternative forms

$$4\pi G^F = \begin{Bmatrix} -1/r' + \mathcal{H} \\ 1/r' + H \end{Bmatrix} \tag{12}$$

with r' given by (1b). The alternative decompositions $4\pi G^F = -1/r' + \mathcal{H}$ and $4\pi G^F = 1/r' + H$ are shown further on to be appropriate for $F = 0$ and $F > 0$, respectively. Thus, (10) and (12) yield

$$4\pi G = \begin{Bmatrix} -1/r - 1/r' + \mathcal{H} \\ -1/r + 1/r' + H \end{Bmatrix} \quad \text{if} \quad \begin{Bmatrix} F = 0 \\ F > 0 \end{Bmatrix} \tag{13a}$$

Expressions (2c) and (11) show that the free-surface components $\mathcal{H}$ and H in (13a) are given by the Fourier superposition of elementary waves

$$\mathcal{F} = \lim_{\varepsilon \to +0} \frac{1}{\pi} \int_{-\infty}^{\infty} d\beta \int_{-\infty}^{\infty} d\alpha \, \frac{A}{D_\varepsilon} \, e^{k(\zeta + z)} \mathcal{E} \tag{13b}$$

with D_ε given by (4) and

$$\mathcal{F} = \begin{Bmatrix} \mathcal{H} \\ H \end{Bmatrix} \quad A = \begin{Bmatrix} f^2/k \\ 1 \end{Bmatrix} \quad \text{if} \quad \begin{Bmatrix} F = 0 \\ F > 0 \end{Bmatrix} \tag{13c}$$

In the special case of wave diffraction-radiation without forward speed, (13c) yields $A = 1$ if $k = f^2$, i.e. at the dispersion curve defined by the dispersion relation $D = 0$.

Two fundamental boundary-integral representations

Consider the basic problem of determining the flow, inside a free-surface potential-flow region, that corresponds to a given flow at a surface Σ bounding the potential-flow region. Here, the boundary surface Σ stands for $\Sigma = \Sigma^H \cup \Sigma^W$ where the surface Σ^H is an arbitrary control surface outside the viscous boundary layer that surrounds the hull of a ship (or other body, e.g. an offshore structure) at or below the free surface, and the surface Σ^W represents the outer edge of the viscous wake trailing the ship or a control surface outside the viscous wake. If viscous effects are ignored, Σ^H may be taken as the wetted surface of the ship hull. For a ship equipped with lifting surfaces, e.g. a sailboat, Σ^W includes the two sides of every vortex sheet behind the ship. For a multihull ship, the hull+wake surface Σ consists of several component surfaces, which correspond to the separate hull components of the ship and their wakes.

Σ may intersect the mean free-surface plane $\zeta = 0$ or may be a closed surface entirely located below the plane $\zeta = 0$. In the former case, Σ is bounded upward by its intersection curve Γ with the plane $\zeta = 0$. The unit vector $\vec{n} = (n^x, n^y, n^z)$ normal to the boundary surface Σ points outside Σ, i.e. inside the flow domain. The unit vector $\vec{t} = (t^x, t^y, 0)$ tangent to the boundary curve Γ is oriented clockwise (looking down). The unit vector normal to Γ in the plane $\zeta = 0$ points inside the flow domain, like $\vec{n}$, and is given by $\vec{\nu} = (-t^y, t^x, 0)$.

A classical fundamental result of potential-flow theory is that the velocity potential ϕ within a potential-flow region bounded by a surface Σ is explicitly defined in terms of the values of the potential ϕ and its normal derivative $\partial\phi/\partial n = \nabla\phi \cdot \vec{n} = \vec{u} \cdot \vec{n}$ at the boundary surface Σ. This fundamental boundary-integral representation — called potential representation because it defines the potential ϕ — and related boundary-integral representations that define ϕ within a potential-flow region in terms of boundary distributions of sources or normal dipoles form the basis of numerous panel methods reported in the ship and offshore-structure hydrodynamics literature to compute linear free-surface potential flows using free-surface Green functions.

Another fundamental boundary-integral representation — given in Noblesse (2000) and called velocity representation — explicitly defines the velocity $\vec{u}$ within a potential-flow region in terms of the velocity $\vec{u}$ at the boundary surface Σ. Thus, the velocity representation does not involve the potential ϕ. This property is a major difference between the velocity representation and the potential representation. The velocity representation can therefore be used to couple a viscous flow, for which a velocity potential cannot be defined, and a potential flow in a direct manner, i.e.

without having to solve an integral equation as is necessary if the potential representation is used. Specifically, the potential representation requires a two-step procedure : an integral equation must first be solved to determine ϕ at the boundary surface from the known boundary value of $\partial\phi/\partial n$, and ϕ and $\nabla\phi$ can subsequently be determined at interior points from the boundary values of ϕ and $\partial\phi/\partial n$.

Another important difference between the potential representation and the velocity representation is that the velocity representation defines $\vec{u}$ in terms of first derivatives of the Green function G, whereas $\vec{u}$ can only be obtained from the potential representation using either analytical differentiation of the potential representation, which involves second-order derivatives of G, or numerical differentiation of ϕ.

The velocity representation and the classical potential representation are given in Noblesse (2000) for generic free-surface potential flows and for four basic classes of flows corresponding to (i) an infinitely rigid or soft free-surface plane, (ii) diffraction-radiation of time-harmonic water waves without forward speed, (iii) steady ship waves, and (iv) time-harmonic ship waves (diffraction-radiation with forward speed). The classical potential representation and the velocity representation are given here for diffraction-radiation of time-harmonic water waves without forward speed, steady ship waves, and time-harmonic ship waves. The potential ϕ and the velocity $\vec{u}$ can be expressed as

$$\left.\begin{aligned} \phi &= \phi^R + \phi^R_* + \phi^{\mathcal{H}} - \phi^p \\ \vec{u} &= \vec{u}^R + \vec{u}^R_* + \vec{u}^{\mathcal{H}} + \vec{u}^{\mathcal{H}}_f - \vec{u}^p \end{aligned}\right\} \quad \text{if } F = 0 \tag{14a}$$

$$\left.\begin{aligned} \phi &= \phi^R - \phi^R_* + \phi^H + \phi^H_F - \phi^p \\ \vec{u} &= \vec{u}^R - \vec{u}^R_* + \vec{u}^H + \vec{u}^H_F - \vec{u}^p \end{aligned}\right\} \quad \text{if } f = 0 \tag{14b}$$

$$\left.\begin{aligned} \phi &= \phi^R - \phi^R_* + \phi^H + \phi^H_F + \phi^H_\tau - \phi^p \\ \vec{u} &= \vec{u}^R - \vec{u}^R_* + \vec{u}^H + \vec{u}^H_F + \vec{u}^H_\tau + \vec{u}^H_f - \vec{u}^p \end{aligned}\right\} \quad \text{if } fF > 0 \tag{14c}$$

The components ϕ^R, $\vec{u}^R$ and ϕ^R_*, $\vec{u}^R_*$ in the potential and velocity representations (14) stem from the Rankine components in the Rankine-Fourier decompositions (13a) of the Green functions associated with the free-surface boundary conditions (3). The Rankine components in (14) are given by surface distributions of elementary Rankine singularities $1/r$ and $1/r'$. Specifically, the

Rankine component ϕ^R, $\vec{u}^R$ is given by

$$4\pi \begin{Bmatrix} -\phi^R \\ u^R \\ v^R \\ w^R \end{Bmatrix} = \int_\Sigma d\mathcal{A} \begin{Bmatrix} -(\vec{u}\cdot\vec{n})\,R + \phi\,(n^x R_x + n^y R_y + n^z R_z) \\ -(\vec{u}\cdot\vec{n})\,R_x - (\vec{u}\times\vec{n})^z\,R_y + (\vec{u}\times\vec{n})^y\,R_z \\ -(\vec{u}\cdot\vec{n})\,R_y - (\vec{u}\times\vec{n})^x\,R_z + (\vec{u}\times\vec{n})^z\,R_x \\ -(\vec{u}\cdot\vec{n})\,R_z - (\vec{u}\times\vec{n})^y\,R_x + (\vec{u}\times\vec{n})^x\,R_y \end{Bmatrix} \tag{15a}$$

with $R = -1/r$. The Rankine component ϕ_*^R, $\vec{u}_*^R$ is given by

$$4\pi \begin{Bmatrix} -\phi_*^R \\ u_*^R \\ v_*^R \\ -w_*^R \end{Bmatrix} = \int_\Sigma d\mathcal{A} \begin{Bmatrix} -(\vec{u}\cdot\vec{n})\,R^* + \phi\,(n^x R_x^* + n^y R_y^* + n^z R_z^*) \\ -(\vec{u}\cdot\vec{n})\,R_x^* - (\vec{u}\times\vec{n})^z\,R_y^* + (\vec{u}\times\vec{n})^y\,R_z^* \\ -(\vec{u}\cdot\vec{n})\,R_y^* - (\vec{u}\times\vec{n})^x\,R_z^* + (\vec{u}\times\vec{n})^z\,R_x^* \\ -(\vec{u}\cdot\vec{n})\,R_z^* - (\vec{u}\times\vec{n})^y\,R_x^* + (\vec{u}\times\vec{n})^x\,R_y^* \end{Bmatrix} \tag{15b}$$

with $R^* = -1/r'$.

The components $\phi^{\mathcal{H}}$, $\vec{u}^{\mathcal{H}}$ and ϕ^H, $\vec{u}^H$ in the potential and velocity representations (14) are defined in terms of the functions $\mathcal{H}$ and H, which account for free-surface effects. The free-surface component $\phi^{\mathcal{F}}$, $\vec{u}^{\mathcal{F}}$ — where $\mathcal{F}$ stands for either $\mathcal{H}$ or H — is given by

$$4\pi \begin{Bmatrix} -\phi^{\mathcal{F}} \\ u^{\mathcal{F}} \\ v^{\mathcal{F}} \\ -w^{\mathcal{F}} \end{Bmatrix} = \int_\Sigma d\mathcal{A} \begin{Bmatrix} -(\vec{u}\cdot\vec{n})\,\mathcal{F} + \phi\,(n^x \mathcal{F}_x + n^y \mathcal{F}_y + n^z \mathcal{F}_z) \\ -(\vec{u}\cdot\vec{n})\,\mathcal{F}_x - (\vec{u}\times\vec{n})^z\,\mathcal{F}_y + (\vec{u}\times\vec{n})^y\,\mathcal{F}_z \\ -(\vec{u}\cdot\vec{n})\,\mathcal{F}_y - (\vec{u}\times\vec{n})^x\,\mathcal{F}_z + (\vec{u}\times\vec{n})^z\,\mathcal{F}_x \\ -(\vec{u}\cdot\vec{n})\,\mathcal{F}_z - (\vec{u}\times\vec{n})^y\,\mathcal{F}_x + (\vec{u}\times\vec{n})^x\,\mathcal{F}_y \end{Bmatrix} \tag{16}$$

Expressions (15) and (16) involve source and vortex distributions over the boundary surface Σ with respective strengths given by the normal component $\vec{u}\cdot\vec{n}$ and the tangential component $\vec{u}\times\vec{n}$ of the velocity at Σ. The velocity components in (15) and (16) only involve the first derivatives ∇R, ∇R^*, $\nabla \mathcal{F}$.

The component $\vec{u}_f^{\mathcal{H}}$ in (14a), the component ϕ_F^H, $\vec{u}_F^H$ in (14b) and (14c), and the components ϕ_τ^H, $\vec{u}_\tau^H$ and $\vec{u}_f^H$ in (14c) are given by distributions over the boundary curve Γ. Specifically, the component $\vec{u}_f^{\mathcal{H}}$ in (14a) is given by

$$4\pi \begin{Bmatrix} u_f^{\mathcal{H}} \\ v_f^{\mathcal{H}} \\ w_f^{\mathcal{H}} \end{Bmatrix} = \int_\Gamma d\mathcal{L}\ \phi \begin{Bmatrix} t^y\,\mathcal{H}_z \\ -t^x\,\mathcal{H}_z \\ t^y\,\mathcal{H}_x - t^x\,\mathcal{H}_y \end{Bmatrix} \tag{17a}$$

The component ϕ_F^H , $\vec{u}_F^H$ in (14b) and (14c) is given by

$$4\pi \begin{Bmatrix} -\phi_F^H \\ u_F^H \\ v_F^H \\ -w_F^H \end{Bmatrix} = F^2 \int_\Gamma d\mathcal{L} \begin{Bmatrix} (\vec{u}\cdot\vec{\nu})\,(t^y)^2 H - (\vec{u}\cdot\vec{t})\,t^x t^y H + \phi\, t^y H_x \\ (\vec{u}\cdot\vec{\nu})\,(t^y)^2 H_x - (\vec{u}\cdot\vec{t})\,t^x t^y H_x \\ (\vec{u}\cdot\vec{\nu})\,(t^y)^2 H_y - (\vec{u}\cdot\vec{t})\,(t^x t^y H_y + H_x) \\ (\vec{u}\cdot\vec{\nu})\,(t^y)^2 H_z - (\vec{u}\cdot\vec{t})\,(t^x t^y H_z - H_{xy}^z) \end{Bmatrix} \tag{17b}$$

The components ϕ_τ^H , $\vec{u}_\tau^H$ and $\vec{u}_f^H$ in (14c) are given by

$$4\pi \begin{Bmatrix} \phi_\tau^H \\ u_\tau^H \\ v_\tau^H \\ w_\tau^H \end{Bmatrix} = i\,2\tau \int_\Gamma d\mathcal{L} \begin{Bmatrix} \phi\, t^y H \\ 0 \\ \vec{u}\cdot\vec{t}\; H \\ \vec{u}\cdot\vec{t}\; H_y^z \end{Bmatrix} \tag{17c}$$

$$4\pi \begin{Bmatrix} u_f^H \\ v_f^H \\ w_f^H \end{Bmatrix} = f^2 \int_\Gamma d\mathcal{L}\; \phi \begin{Bmatrix} t^y H \\ -t^x H \\ t^y H_x^z - t^x H_y^z \end{Bmatrix} \tag{17d}$$

The function H^z in (17b)-(17d) is defined as

$$H^z(\xi - x, \eta - y, \zeta + z) = \int_{-\infty}^{z} dt\; H(\xi - x, \eta - y, \zeta + t)$$

The function H_{xy}^z in (17b) is comparable to the first derivative ∇H of H (the functions H_{xy}^z and ∇H have similar behaviors in the near field and the far field). The functions H_x^z and H_y^z in (17c) and (17d) likewise are comparable to the function H.

Finally, the component ϕ^p, $\vec{u}^p$ associated with the nonhomogeneous term p in the free-surface conditions (3) is given by

$$4\pi \begin{Bmatrix} \phi^p \\ u^p \\ v^p \\ w^p \end{Bmatrix} = \int_{\Sigma^F} d\mathcal{A}\; p \begin{Bmatrix} H \\ -H_x \\ -H_y \\ H_z \end{Bmatrix} = \int_{\Sigma^F} d\mathcal{A}\; p \begin{Bmatrix} H \\ H_\xi \\ H_\eta \\ H_\zeta \end{Bmatrix} \tag{18}$$

where Σ^F stands for the mean free surface.

The velocity components $\vec{u}_F^H$ and $\vec{u}_\tau^H$ defined by (17b) and (17c) involve the normal component $\vec{u}\cdot\vec{\nu}$ and/or the tangential component $\vec{u}\cdot\vec{t}$ of the velocity $\vec{u}$ at the boundary curve Γ. Expressions (17a) and (17d) for the components $\vec{u}_f^{\mathcal{H}}$ and $\vec{u}_f^H$ involve the potential ϕ, which is defined in terms

of the velocity $\vec{u}$ by the free-surface conditions (3c) and (3a). In the special cases $f=0$ and $F=0$, (14c) can be verified to be identical to (14b) and (14a) as expected.

The boundary-integral representations (14)-(18) are obtained in Noblesse (2000) using elementary identities in vector calculus. Specifically, the divergence theorem is used in the 3D flow region bounded by the closed surface $\Sigma \cup \Sigma^\infty \cup \Sigma^F$. Here, Σ^∞ represents a large outer boundary surface that surrounds the previously-defined hull+wake inner boundary surface Σ, and Σ^F stands for the portion of the mean free-surface plane $z=0$ that is bounded by the intersection curves Γ and Γ^∞ between the plane $z=0$ and the inner and outer boundary surfaces Σ and Σ^∞. Stokes' theorem is also used in the 2D free-surface region Σ^F bounded by $\Gamma \cup \Gamma^\infty$ for the purpose of expressing the contribution of the free surface Σ^F in terms of a line integral around the inner boundary curve Γ. Thus, the line integrals (17) and the corresponding components in (14) are associated with the contribution of the mean free-surface plane Σ^F outside the boundary surface Σ. The flow representations (14)-(18), given here for deep water, can be extended to uniform finite water depth, and indeed can be extended to a broader class of problems involving dispersive waves that propagate in the presence of a planar boundary.

The classical Green-function method

The potential and velocity representations (14)-(18) provide a mathematical basis for computing steady ship waves and wave diffraction-radiation by offshore structures and ships using the free-surface Green functions (13). Free-surface effects in the boundary-integral representations (14)-(18) and the corresponding free-surface Green functions are represented by the components $\mathcal{H}$ and H given by the double Fourier integral (13b).

The special case $F=0$ is sufficiently simple that the double Fourier integral (13b) can be easily evaluated. Specifically, the function $\mathcal{H}$ is expressed in Noblesse (1982) as

$$\mathcal{H} = \mathcal{W} + \mathcal{L} \tag{19a}$$

where $\mathcal{W}$ and $\mathcal{L}$ respectively represent a system of circular waves and a local flow disturbance. The wave component $\mathcal{W}$ is given by the remarkably simple expression

$$\mathcal{W} = -2\pi f^2 \left[\tilde{E}_0(f^2 h) + i\, J_0(f^2 h) \right] \exp\left[f^2(\zeta + z) \right] \tag{19b}$$

obtained in Noblesse (1982). Here, $h = \sqrt{(\xi - x)^2 + (\eta - y)^2}$, J_0 is the usual Bessel function and $\tilde{E}_0$ is the Weber function defined in chapter 12 of Abramowitz & Stegun (1965). The functions $\tilde{E}_0$

and J_0 are infinitely differentiable and can be evaluated quite efficiently. The local flow component $\mathcal{L}$ in (19a) can be evaluated in a highly efficient manner using a simple analytical approximation based on the nearfield and farfield analytical approximations given in Noblesse (1982), or more accurately using table interpolation as in Ponizy et al. (1994).

Simple analytical expressions like (19b) are not available if $F>0$, i.e. for the free-surface Green functions associated with steady and time-harmonic ship waves, because forward-speed effects introduce considerable mathematical difficulties. More precisely, the classical Green-function approach requires practical methods for performing two necessary basic tasks: (i) evaluation of the free-surface component H in (13a) and its gradient ∇H, i.e. evaluation of the double Fourier integral (13b), and (ii) integration of H and ∇H over a hull panel and a waterline segment. Both of these two basic tasks are difficult because the functions H and ∇H are singular and highly oscillatory in the limit $r' \to 0$. Although the evaluation and the subsequent hull-panel integration of H and ∇H have been considered in numerous studies in the ship-hydrodynamics literature, no simple practical method of performing these two basic tasks appears to be available yet. Indeed, the integral representations of the Green functions associated with the free-surface boundary conditions for steady and time-harmonic ship waves given, for instance, in Noblesse (1981) and Chen (1999) are relatively complicated and ill-suited for efficient flow calculations. Free-surface effects associated with the Fourier component H defined by the double Fourier integral (13b) can be analyzed more simply and effectively using the Fourier-Kochin approach expounded in Noblesse and Yang (1995) and Noblesse (2000). This approach is summarized below.

Fourier-Kochin representation of free-surface effects

The order in which the tasks of evaluating the functions H and ∇H (a Fourier integration) and of integrating H and ∇H over hull panels and waterline segments (a space integration) are performed is reversed in the Fourier-Kochin approach. Specifically, expression (13b) for the free-surface component H is substituted into (16)-(18), and the integrations with respect to the space variables (x, y, z) and the Fourier variables (α, β) are permuted. Thus, space integration is performed first, and Fourier integration is performed subsequently in the Fourier-Kochin approach.

An evident advantage of the Fourier-Kochin approach is that the space integration, which is very complex within the classical Green-function method (because the functions H and ∇H are singular and highly oscillatory as already noted), is a trivial task within the Fourier-Kochin method. Indeed,

the Fourier-Kochin space integration consists in evaluating spectrum functions, defined below by (22), given by distributions of elementary waves over the surface $\Sigma \cup \Gamma \cup \Sigma^F$. The Fourier integration, on the other hand, is simpler in an important respect but more complicated in another respect, within the Fourier-Kochin approach than the classical Green-function method, as is explained further on.

The Fourier components in the boundary-integral representations (14) are now defined in terms of Fourier-Kochin distributions of elementary waves. The Fourier components $\phi^{\mathcal{H}}$, $\vec{u}^{\mathcal{H}}$, $\vec{u}_f^{\mathcal{H}}$, ϕ^p, $\vec{u}^p$ in the representation (14a) of time-harmonic flows without forward speed can be expressed as

$$4\pi \begin{Bmatrix} \phi^{\mathcal{H}} - \phi^p \\ u^{\mathcal{H}} + u_f^{\mathcal{H}} - u^p \\ v^{\mathcal{H}} + v_f^{\mathcal{H}} - v^p \\ w^{\mathcal{H}} + w_f^{\mathcal{H}} - w^p \end{Bmatrix} = \lim_{\varepsilon \to +0} \frac{1}{\pi} \int_{-\infty}^{\infty} d\beta \int_{-\infty}^{\infty} d\alpha \begin{Bmatrix} 1 \\ -i\,\alpha \\ -i\,\beta \\ k \end{Bmatrix} S^W \frac{f^2 \mathcal{E}^*}{k\, D_\varepsilon} \tag{20a}$$

Here, $D_\varepsilon = f^2 - k + i f \varepsilon$ in accordance with (4), $\mathcal{E}^*$ is given by

$$\mathcal{E}^* = e^{k\zeta - i(\alpha\xi + \beta\eta)}$$

and the function S^W is the wave-spectrum function defined in the next section. If $F > 0$, the Fourier components in (14b) and (14c) can be expressed as

$$4\pi \begin{Bmatrix} \phi^H + \phi_F^H + \phi_\tau^H - \phi^p \\ u^H + u_F^H + u_f^H - u^p \\ v^H + v_F^H + v_f^H + v_\tau^H - v^p \\ w^H + w_F^H + w_f^H + w_\tau^H - w^p \end{Bmatrix} = \lim_{\varepsilon \to +0} \frac{1}{\pi} \int_{-\infty}^{\infty} d\beta \int_{-\infty}^{\infty} d\alpha\, \vec{S}\, \frac{\mathcal{E}^*}{D_\varepsilon} \tag{20b}$$

where D_ε is given by (4), and $\vec{S}$ is defined as

$$\vec{S} = \begin{Bmatrix} 1 \\ -i\,\alpha \\ -i\,\beta \\ k \end{Bmatrix} S^W - \frac{D}{k} \begin{Bmatrix} S_*^\phi \\ -i\,\beta\, S_*^t / k \\ i\,\alpha\, S_*^t / k \\ 0 \end{Bmatrix} \tag{20c}$$

Here, $D = (f - F\alpha)^2 - k$ and the wave-spectrum function S^W is given in the next section.

The Fourier-Kochin representation of free-surface effects given by (20) and expressions (21) and (22) for the wave-spectrum function S^W is obtained in Noblesse (2000) by substituting (13b) into (16)-(18), exchanging the order in which the integrations with respect to the Fourier variables

$(\alpha\,,\beta)$ and the space variables $(x\,,y\,,z)$ are performed, and performing several mathematical transformations of the resulting spectrum functions.

Wave-spectrum functions

The wave-spectrum function S^W in (20a) and (20c) is defined in Noblesse (2000) as

$$S^W = \left\{ \begin{array}{c} S + S^{\phi}_{*} \\ S + F^2 S^F \\ S + \frac{f^2}{k}\, S^{\phi}_{*} + F^2 S^F - \frac{2\tau}{k}\,\frac{\beta}{k}\, S^t_{*} \end{array} \right\} - S^p \quad \text{if} \left\{ \begin{array}{c} F = 0 \\ f = 0 \\ fF > 0 \end{array} \right\} \tag{21}$$

where the five spectrum functions S, S^{ϕ}_{*}, S^t_{*}, S^F, S^p are given by

$$S = \int_{\Sigma} d\mathcal{A}\, [\, \vec{u}\cdot\vec{n} + i\,\frac{\alpha}{k}\,(\,\vec{u}\times\vec{n}\,)^y - i\,\frac{\beta}{k}\,(\,\vec{u}\times\vec{n}\,)^x\,]\, e^{k\,z}\,\mathcal{E}_0 \tag{22a}$$

$$\left\{ \begin{array}{c} S^{\phi}_{*} \\ S^t_{*} \\ S^F \end{array} \right\} = \int_{\Gamma} d\mathcal{L} \left\{ \begin{array}{c} i\,\phi\,(\,\alpha\, t^y - \beta\, t^x\,)/\,k \\ \vec{u}\cdot\vec{t} \\ (\,t^x t^y + \alpha\,\beta/k^2\,)\,\vec{u}\cdot\vec{t} - (t^y)^2\,\vec{u}\cdot\vec{\nu} \end{array} \right\} \mathcal{E}_0 \tag{22b}$$

$$S^p = \int_{\Sigma^F} d\mathcal{A}\; p\; \mathcal{E}_0 \tag{22c}$$

$$\text{with} \qquad \mathcal{E}_0 = e^{\,i\,(\,\alpha\, x + \beta\, y\,)} \tag{22d}$$

The spectrum function S, the spectrum functions S^{ϕ}_{*}, S^t_{*}, S^F, and the spectrum function S^p are respectively given by distributions of elementary waves over the boundary surface Σ, the boundary curve Γ, and the mean free surface Σ^F. The spectrum functions S, S^t_{*}, S^F are defined in terms of the normal components $\vec{u}\cdot\vec{n}$, $\vec{u}\cdot\vec{\nu}$ and the tangential components $\vec{u}\times\vec{n}$, $\vec{u}\cdot\vec{t}$ of the velocity $\vec{u}$ at the boundary surface Σ and the boundary curve Γ. The spectrum function S^{ϕ}_{*} is defined in terms of the potential ϕ.

In the special case $f = 0$, i.e. for steady flow, the spectrum function S^W is defined by (21) in terms of the spectrum functions S and S^F, which do not involve the potential ϕ and are defined directly in terms of the velocity $\vec{u}$. If $f > 0$, (21) shows that S^W involves the spectrum function S^{ϕ}_{*} defined in terms of the potential ϕ, although the free-surface boundary conditions (3) can be used to express ϕ in terms of $\vec{u}$.

Green functions and super Green functions

Expressions (21) and (22) show that the spectrum functions S^W and $\vec{S}$ in (20) are given by distributions of elementary waves over the surface $\Sigma \cup \Gamma \cup \Sigma^F$. This surface can be divided into a set of patches associated with reference points $(x_p\,, y_p\,, z_p \leq 0)$ located near the centroids of the patches. The spectrum functions S^W and $\vec{S}$ in (20) are then of the form

$$\sum_{p=1}^{p=N} S_p \; e^{k\,z_p + i\,(\alpha\,x_p + \beta\,y_p)}$$

where summation is performed over all the N patches that represent the surface $\Sigma \cup \Gamma \cup \Sigma^F$, and S_p is a slowly-varying function of α and β. Expressions (20a) and (20b) therefore involve double Fourier integrals of the type

$$\lim_{\varepsilon \to +0} \int_{-\infty}^{\infty} d\beta \int_{-\infty}^{\infty} d\alpha \; \frac{A_p}{D_\varepsilon} \; e^{k\,(\zeta + z_p) - i\,[\alpha\,(\xi - x_p) + \beta\,(\eta - y_p)]}$$

where A_p is not a rapidly oscillatory function of α and β. This Fourier integral is similar to the Fourier integral (11a) that defines the free-surface component G^F in the ship-motion Green function. Indeed, (11a) and (2b) show that G^F is defined in terms of the Fourier integral

$$\lim_{\varepsilon \to +0} \int_{-\infty}^{\infty} d\beta \int_{-\infty}^{\infty} d\alpha \; \frac{A^F}{D_\varepsilon} \; e^{k\,(\zeta + z) - i\,[\alpha\,(\xi - x) + \beta\,(\eta - y)]}$$

Expression (4a) shows that the foregoing Fourier integrals are of the form

$$\mathcal{G} = \lim_{\varepsilon \to +0} \int_{-\infty}^{\infty} d\beta \int_{-\infty}^{\infty} d\alpha \; \frac{A \; e^{-i\,(X\,\alpha + Y\,\beta)}}{D + i\,\varepsilon\,D'} \tag{23}$$

with $A = A_p\, e^{k\,(\zeta + z_p)}$ or $A = A^F e^{k\,(\zeta + z)}$. A function $\mathcal{G}$ associated with a distribution of singularities is called a super Green function because of its similarities and differences with usual Green functions, which correspond to a point source.

The amplitude function A^F corresponding to a point source is simpler than the amplitude function A_p associated with a Fourier-Kochin distribution of singularities over a patch. In fact, (13c) shows that the amplitude function corresponding to the Rankine-Fourier decompositions (13a) of the Green functions associated with the free-surface conditions (3) is equal to 1 if $F > 0$ or f^2/k if $F = 0$. Thus, the Fourier integral (23) is, in this respect, more complicated for a distribution of singularities than for a point source, i.e. for the Fourier-Kochin approach than for the classical Green-function method.

The amplitude function A in (23) vanishes exponentially in the limit $k \to \infty$ if $\zeta + z_p < 0$ or $\zeta + z < 0$. However, the amplitude functions corresponding to a point source and a distribution

of sources differ in an important respect in the limiting case $\zeta + z_p = 0$ or $\zeta + z = 0$. Specifically, the amplitude function A corresponding to a distribution of singularities over the free-surface plane $z = 0$ vanishes as $k \to \infty$ in all cases (i.e. even if $\zeta = 0$), whereas $A = 1$ for a point source if $F > 0$ and $\zeta + z = 0$. This difference between the Fourier integrals associated with a point source and a distribution of sources corresponds to the fact that the component that accounts for free-surface effects is singular for a point source in the limit $\zeta + z \to 0$ but is finite for a distribution of singularities. Thus, the Fourier integral (23) is in this respect simpler for a distribution of singularities than for a point source.

A reliable and practical method for evaluating super Green functions of the type defined by (23) evidently is a critical requirement of the Fourier-Kochin representation of free-surface effects. This fundamental issue has been considered for a generic dispersion function $D + i\varepsilon D'$ and a generic amplitude function A, i.e. for a broad class of dispersive waves and arbitrary distributions of singularities, in several studies. The most important result of these studies of generic super Green functions — obtained by the author in cooperation with Dr. Chi Yang and first given in Noblesse and Chen (1995) — is a formal decomposition of the generic super Green function (23) into wave and local components, and a remarkably simple Fourier representation of the wave component. Alternative Fourier representations of the local component in this wave+local decomposition are given in Noblesse and Yang (1996), Noblesse and Chen (1997), and Noblesse et al. (1999). The most practical of these alternative representations is that given in Noblesse and Chen (1997). This study and Noblesse et al. (1999) are summarized below.

Practical representation of generic super Green functions

The double Fourier integral (23) has been considered in numerous studies of free-surface Green functions. These studies rely on integration contours in the complex Fourier plane $\alpha = \alpha_r + i\,\alpha_i$, or alternatively in the complex Fourier planes $\beta = \beta_r + i\,\beta_i$ or $k = k_r + i\,k_i$, in the manner explained in Noblesse (1981). A different approach is used here and in the previously-listed studies of generic super Green functions : the Fourier representation (23) is analyzed directly, i.e. without introducing a contour of integration, in the real Fourier space $(\alpha\,,\beta)$.

The double Fourier integral (23) can be expressed in the basic form

$$\mathcal{G} = \mathcal{G}_2 + \mathcal{G}_1 \tag{24a}$$

Here, $\mathcal{G}_2$ is the double Fourier integral

$$\mathcal{G}_2 = \int_{-\infty}^{\infty} d\beta \int_{-\infty}^{\infty} d\alpha \, \frac{A}{D} \, e^{-i(X\alpha + Y\beta)} \tag{24b}$$

obtained by formally setting $\varepsilon = 0$ in (23). Noblesse et al. (1999) show that $\mathcal{G}_1 = \mathcal{G} - \mathcal{G}_2$ can be expressed in terms of single Fourier integrals along the dispersion curve(s) defined by the dispersion relation $D(\alpha, \beta) = 0$:

$$\mathcal{G}_1 = -i\pi \sum_{D=0} \int_{D=0} ds \, \frac{\text{sign}(D')}{\|\nabla D\|} \, A \, e^{-i(X\alpha + Y\beta)} \tag{24c}$$

$\|\nabla D\| = \sqrt{D_\alpha^2 + D_\beta^2}$ where D_α and D_β are the derivatives of the dispersion function D with respect to the Fourier variables α and β, and ds stands for the differential element of arc length along a dispersion curve.

A fundamental result of the theory of Fourier transforms, given in Lighthill (1970), is that the behavior of a function $f(x)$ in the farfield $x \to \infty$ is determined by the dominant singularities of its Fourier transform. Thus, the dominant farfield features of the function $\mathcal{G}_2$ defined by (24b), i.e. the farfield waves contained in $\mathcal{G}_2$, stem from the dispersion curves defined by the dispersion relation $D = 0$. Specifically, Noblesse et al. (1999) yield

$$\mathcal{G}_2 \sim \mathcal{G}_2^W = -i\pi \sum_{D=0} \int_{D=0} ds \, \frac{\text{erf}(\psi)}{\|\nabla D\|} \, A \, e^{-i(X\alpha + Y\beta)} \tag{25a}$$

in the farfield limit $X^2 + Y^2 \to \infty$. Here, erf is the usual error function and ψ is defined below. The basic decomposition (24a) and the farfield approximation (25a) yield

$$\mathcal{G} \sim \mathcal{G}^W = \mathcal{G}_1 + \mathcal{G}_2^W \tag{25b}$$

as $X^2 + Y^2 \to \infty$. Expressions (24c) and (25a) yield

$$\mathcal{G}^W = -i\pi \sum_{D=0} \int_{D=0} ds \, \frac{\text{sign}(D') + \text{erf}(\psi)}{\|\nabla D\|} \, A \, e^{-i(X\alpha + Y\beta)} \tag{26a}$$

The function ψ in (26a) is given by

$$\psi = \frac{k(XD_\alpha + YD_\beta)}{\sigma \|\nabla D\|} \tag{26b}$$

where $\sigma \approx 1$ is a positive real number. The error function $\text{erf}(\psi)$ becomes

$$\text{erf}(\psi) \sim \text{sign}(XD_\alpha + YD_\beta) \text{ as } X^2 + Y^2 \to \infty \tag{26c}$$

The term sign(D') in (26a), which stems from the component $\mathcal{G}_1$ in (24a), ensures that the radiation condition is satisfied.

In the nearfield, the super Green function $\mathcal{G}$ can be expressed as the sum of the wave component $\mathcal{G}^W$ given by (26) and a local component $\mathcal{G}^L$:

$$\mathcal{G} = \mathcal{G}^W + \mathcal{G}^L \tag{27}$$

Expressions (24a) and (25b) show that the local component $\mathcal{G}^L = \mathcal{G} - \mathcal{G}^W$ is given by

$$\mathcal{G}^L = \mathcal{G}_2 - \mathcal{G}_2^W$$

Alternative representations of the local component $\mathcal{G}^L$ in the fundamental decomposition (27) into wave and local components are given in Noblesse and Yang (1996), Noblesse and Chen (1997), and Noblesse et al. (1999). The latter study considers special cases, corresponding to simple open and closed dispersion curves, and the general case of arbitrary dispersion curves. A simpler representation that is valid for arbitrary dispersion curves is (see Appendix 3)

$$\mathcal{G}^L = \int_{-\infty}^{\infty} d\beta \int_{-\infty}^{\infty} d\alpha \, (A - \sum_{D=0} E_j \, A_j) \, \frac{e^{-i(X\alpha + Y\beta)}}{D} \tag{28a}$$

Summation in (28a) is performed over all the dispersion curves, which are identified by the subscript j, and E_j is defined as

$$E_j = \frac{\|\nabla D\|}{\|\nabla D\|_j} \exp[\, \frac{-\sigma^2 D^2}{4\, k_j^2 \, \|\nabla D\|_j^2} + i\, X(\alpha - \alpha_j - \frac{D D_\alpha^j}{\|\nabla D\|_j^2}) + i\, Y(\beta - \beta_j - \frac{D D_\beta^j}{\|\nabla D\|_j^2}) \,] \tag{28b}$$

The subscript or superscript j in (28) indicates evaluation at the j^{th} dispersion curve; e.g. A_j stands for the value of the amplitude function A at the j^{th} dispersion curve.

The local component $\mathcal{G}^L$ defined by (28) can be further decomposed as in Noblesse and Chen (1997) :

$$\mathcal{G}^L = \mathcal{G}_*^L + \mathcal{G}_D^L \tag{29a}$$

Here, the component $\mathcal{G}_*^L$ is defined as

$$\mathcal{G}_*^L = \int_{-\infty}^{\infty} d\beta \int_{-\infty}^{\infty} d\alpha \, \frac{1-E}{D} \, A \, e^{-i(X\alpha + Y\beta)} \tag{29b}$$

$$\text{with} \qquad E = \exp(\, \frac{-\sigma^2 D^2}{4\, k^2 \, \|\nabla D\|^2} \,) \tag{29c}$$

The component $\mathcal{G}_D^L$ in (29a) is then given by

$$\mathcal{G}_D^L = \int_{-\infty}^{\infty} d\beta \int_{-\infty}^{\infty} d\alpha \, \frac{E\, A - \sum E_j \, A_j}{D} \, e^{-i(X\alpha + Y\beta)} \tag{29d}$$

where the functions E_j and E are given by (28b) and (29c). The component $\mathcal{G}_*^L$ defined by (29b) accounts for the contribution of the entire Fourier plane except the regions near the dispersion curves. The contribution of these dispersion strips is given by the component $\mathcal{G}_D^L$ defined by (29d). The integrand of the double Fourier integral (29b) vanishes at a dispersion curve $D=0$, and this Fourier integral can be evaluated simply and very efficiently if the amplitude function A is not rapidly oscillatory, as is assumed here. The integrand of (29d) is finite at a dispersion curve, and the component $\mathcal{G}_D^L$ can also be evaluated without difficulty.

In fact, Noblesse and Chen (1997) shows that this component can be approximated by the single Fourier integrals

$$\mathcal{G}_D^L \approx \frac{2\sqrt{\pi}}{\sigma} \sum_{D=0} \int_{D=0} ds \, \frac{k\, e^{-\psi^2}}{\|\nabla D\|} \left(\frac{\partial A}{\partial \nu} - CA \right) e^{-i(X\alpha + Y\beta)} \tag{30a}$$

along the dispersion curves $D=0$. Here, ψ is given by (26b) and

$$C = (D_{\alpha\alpha} D_\alpha^2 + 2D_{\alpha\beta} D_\alpha D_\beta + D_{\beta\beta} D_\beta^2)/\|\nabla D\|^3 \tag{30b}$$

Furthermore, $\partial A/\partial \nu$ is the derivative of the amplitude function $A(\alpha, \beta)$ in the direction of the unit vector $\vec{\nu} = \nabla D/\|\nabla D\|$ normal to a dispersion curve in the Fourier plane (α, β). The derivative $\partial A/\partial \nu$ can be determined using analytical or numerical differentiation, i.e.

$$\frac{\partial A}{\partial \nu} = \frac{D_\alpha A_\alpha + D_\beta A_\beta}{\|\nabla D\|} \approx \frac{A(\alpha^+, \beta^+) - A(\alpha^-, \beta^-)}{2\,\delta} \tag{30c}$$

Here, $A(\alpha^\pm, \beta^\pm)$ are the values of the function A at points

$$(\alpha^\pm, \beta^\pm) = (\alpha, \beta) \pm \delta\, (D_\alpha, D_\beta)/\|\nabla D\| \tag{30d}$$

defined via displacements $\pm\delta\,\vec{\nu}$ from a point (α, β) of a dispersion curve.

In summary, (27) and (29a) show that the super Green function $\mathcal{G}$ defined by the singular double Fourier integral (23) can be expressed as

$$\mathcal{G} = \mathcal{G}^W + \mathcal{G}^L = \mathcal{G}^W + \mathcal{G}_D^L + \mathcal{G}_*^L \tag{31}$$

$\mathcal{G}^W$ and $\mathcal{G}_D^L$ are given by the single Fourier integrals (26) and (30), and $\mathcal{G}_*^L$ is defined by the regular double Fourier integral (29b) and (29c). The single Fourier integrals (26a) and (30a) can evidently be combined, as in Noblesse and Chen (1997). The wave component $\mathcal{G}^W$ and the local components $\mathcal{G}_D^L$ and $\mathcal{G}_*^L$ in the representation (31) can be evaluated in a straightforward and highly efficient

manner if the amplitude function A in (23) is not rapidly oscillatory.

Fourier-Kochin representation of nearfield waves

The decomposition (27) shows that the double Fourier integrals (20a) and (20b), which are of the form (23), can be expressed as sums of wave and local components :

$$\left\{ \begin{array}{c} \phi^{\mathcal{H}} - \phi^{p} \\ \vec{u}^{\mathcal{H}} + \vec{u}_f^{\mathcal{H}} - \vec{u}^{p} \end{array} \right\} = \left\{ \begin{array}{c} \phi^{W} + \phi^{L} \\ \vec{u}^{W} + \vec{u}^{L} \end{array} \right\} \tag{32a}$$

$$\left\{ \begin{array}{c} \phi^{H} + \phi_F^{H} + \phi_\tau^{H} - \phi^{p} \\ \vec{u}^{H} + \vec{u}_F^{H} + \vec{u}_\tau^{H} + \vec{u}_f^{H} - \vec{u}^{p} \end{array} \right\} = \left\{ \begin{array}{c} \phi^{W} + \phi^{L} \\ \vec{u}^{W} + \vec{u}^{L} \end{array} \right\} \tag{32b}$$

The wave components in the decompositions (32) are defined by (26a) in terms of single Fourier integrals along the dispersion curves defined by the dispersion relation $D=0$. It follows that the second component on the right side of (20c) does not contribute to the waves contained in (20b).

Specifically, the wave component ϕ^W, $\vec{u}^W$ in (32) is given by

$$4\pi \left\{ \begin{array}{c} \phi^{W} \\ u^{W} \\ v^{W} \\ w^{W} \end{array} \right\} = -i \sum_{D=0} \int_{D=0} \frac{ds}{\|\nabla D\|} \left\{ \begin{array}{c} 1 \\ -i\,\alpha \\ -i\,\beta \\ k \end{array} \right\} \sum_{p=1}^{p=N} [\,\mathrm{sign}(D') + \mathrm{erf}(\psi_p)\,]\, S_p^W \mathcal{E}_p^* \tag{33a}$$

The identity $f^2 = k$ at a dispersion curve $D = 0$, which follows from (5a), was used in (20a). The functions D and D' in (33a) are given by (4b). Summation is performed over all the patches that represent the surface $\Sigma \cup \Gamma \cup \Sigma^F$, as previously explained. The function S_p^W stands for the contribution of patch p to the wave-spectrum function S^W defined by (21) and (22), with the substitutions

$$\left\{ \begin{array}{c} (\,\Sigma\,,\Gamma\,,\Sigma^F\,) \rightarrow (\,\Sigma_p\,,\Gamma_p\,,\Sigma_p^F\,) \\ (\,x\,,y\,,z\,) \rightarrow (\,x - x_p\,,y - y_p\,,z - z_p\,) \end{array} \right\} \tag{33b}$$

performed in (22). The function $\mathcal{E}_p^*$ is given by

$$\mathcal{E}_p^* = e^{(\zeta + z_p)\,k - i\,[\,(\xi - x_p)\,\alpha + (\eta - y_p)\,\beta\,]} \tag{33c}$$

Finally, ψ_p is defined by (26b) as

$$\psi_p = k\,\frac{(\,\xi - x_p\,)\,D_\alpha + (\,\eta - y_p\,)\,D_\beta}{\sigma\,\|\nabla D\|} \tag{33d}$$

In the farfield, we have

$$\mathrm{erf}(\psi_p) \approx \mathrm{sign}[\,(\,\xi - x_p\,)\,D_\alpha + (\,\eta - y_p\,)\,D_\beta\,]$$

and division of the surface $\Sigma \cup \Gamma \cup \Sigma^F$ into patches may not be necessary, as shown in Yang et al. (2000a). In summary, farfield and nearfield waves are defined by (33) in terms of the wave-spectrum function S^W given by (21) and (22).

Time-harmonic ship waves

The dispersion curves in the regions (7) yield distinct contributions to the wave component ϕ^W, $\vec{u}^W$ defined by (33a). If $\tau < 1/4$, ϕ^W and $\vec{u}^W$ can be expressed as

$$\begin{Bmatrix} \phi^W \\ \vec{u}^W \end{Bmatrix} = \begin{Bmatrix} \phi^W_R + \phi^W_{oV} + \phi^W_{iV} \\ \vec{u}^W_R + \vec{u}^W_{oV} + \vec{u}^W_{iV} \end{Bmatrix} \tag{34a}$$

The components $\vec{u}^W_R$, $\vec{u}^W_{oV}$, $\vec{u}^W_{iV}$ respectively correspond to the dispersion curves in the inner region $\alpha_i^- \le \alpha \le \alpha_i^+$ and the outer regions $\alpha \le \alpha_o^-$ and $\alpha_o^+ \le \alpha$. The component $\vec{u}^W_R$ represents a system of ring-like waves, called ring waves. The components $\vec{u}^W_{oV}$ and $\vec{u}^W_{iV}$ represent two systems of V-like waves contained within wedges and called outer-V waves and inner-V waves, respectively. Curves of constant phase (e.g. crest lines) corresponding to the ring waves (thick solid lines), the outer-V waves (dashed lines), and the inner-V waves (thin solid lines) are depicted on the left side of Fig. 3 for $\tau = 0.24$. In the limit $\tau = 0$, the components $\vec{u}^W_R$ and $\vec{u}^W_{oV} + \vec{u}^W_{iV}$ respectively correspond to time-harmonic ring waves (limit $F=0$) and steady ship waves (limit $f=0$).

If $\tau > 1/4$, ϕ^W and $\vec{u}^W$ can be expressed as

$$\begin{Bmatrix} \phi^W \\ \vec{u}^W \end{Bmatrix} = \begin{Bmatrix} \phi^W_{RF} + \phi^W_{iV} \\ \vec{u}^W_{RF} + \vec{u}^W_{iV} \end{Bmatrix} \tag{34b}$$

where $\vec{u}^W_{RF}$ and $\vec{u}^W_{iV}$ are associated with the dispersion curves in the regions $\alpha \le \alpha_i^+$ and $\alpha_o^+ \le \alpha$, respectively. The component $\vec{u}^W_{iV}$ represents a system of inner-V waves qualitatively similar to the inner-V waves in (34a). The component $\vec{u}^W_{RF}$ represents fan-like waves and incomplete ring waves. These waves are also contained within a wedge, and are called ring-fan waves. The system of ring-fan waves can be further divided into two systems of waves : a system of inner-fan waves and a system of partial-ring waves and outer-fan waves, which correspond to the portions $\alpha \le -f/F$ and $-f/F \le \alpha \le \alpha_i^+$ of the dispersion curve $\alpha \le \alpha_i^+$. Constant-phase curves corresponding to the

partial-ring waves and the outer-fan waves (thick solid lines), the inner-fan waves (dashed lines), and the inner-V waves (thin solid lines) are depicted on the right side of Fig. 3 for $\tau = 0.26$.

Expressions for the four basic time-harmonic ship-wave components — i.e. the inner-V waves in (34a) and (34b), the ring-fan waves in (34b), and the outer-V waves and the ring waves in (34a) — can be obtained from (33) and are now given. The inequalities (8) yield $\text{sign}(D') = \text{sign}(f - F\alpha) = 1$ for all the dispersion curves located in the regions defined by (7), except the dispersion curve in the region $\alpha_o^+ \le \alpha$ for which $\text{sign}(D') = -1$. The ship-motion dispersion function, defined by (4b) as $D = (F\alpha - f)^2 - k$, yields $D_\beta = -\beta/k$ and $D_\alpha = -\widehat{\alpha}/k$ with

$$\widehat{\alpha} = \alpha + 2k\,(\tau - F^2\alpha)$$

Expression (33d) then yields $\psi_p = -\varphi_p$ with

$$\varphi_p = k\,\frac{(\xi - x_p)\,\widehat{\alpha} + (\eta - y_p)\,\beta}{\sigma\,\sqrt{\widehat{\alpha}^2 + \beta^2}} \tag{35}$$

The dispersion curves in the three regions $\alpha_o^+ \le \alpha$, $\alpha \le \alpha_i^+$, $\alpha \le \alpha_o^-$ can be defined by the parametric representation

$$\left\{ \begin{array}{c} k = \sqrt{k_0^2 + t^2} \\ \alpha = f/F - \varepsilon\,\sqrt{k}\,/F \\ \beta = \sqrt{k^2 - \alpha^2}\ \text{sign}(t) \end{array} \right\} \tag{36a}$$

where $-\infty \le t < \infty$ and

$$k_0 = \left\{ \begin{array}{c} \alpha_o^+ \\ \alpha_i^+ \\ -\alpha_o^- \end{array} \right\} \qquad \varepsilon = \left\{ \begin{array}{c} -1 \\ 1 \\ 1 \end{array} \right\} \qquad \text{for} \left\{ \begin{array}{c} \text{inner-V} \\ \text{ring-fan} \\ \text{outer-V} \end{array} \right\} \text{waves} \tag{36b}$$

with α_o^+, α_i^+, α_o^- given by (6). $\widehat{\alpha}$ in (35) is then given by

$$\widehat{\alpha} = f/F + \varepsilon\,(2F^2k - 1)\,\sqrt{k}\,/F \tag{36c}$$

Finally, (33a) and the relation $ds/\|\nabla D\| = \varepsilon\,d\alpha/D_\beta = -\varepsilon\,k\,d\alpha/\beta$ yield

$$4\pi \left\{ \begin{array}{c} \phi_\gamma^W \\ u_\gamma^W \\ v_\gamma^W \\ w_\gamma^W \end{array} \right\} = \frac{1}{2F} \int_{-\infty}^{\infty} \frac{dt\ t}{\beta\,\sqrt{k}} \left\{ \begin{array}{c} i \\ \alpha \\ \beta \\ i\,k \end{array} \right\} \sum_{p=1}^{p=N} \left[\,\text{erf}(\varphi_p) - \varepsilon\,\right] S_p^W\,\mathcal{E}_p^* \tag{36d}$$

The subscript γ in ϕ_γ^W and $\vec{u}_\gamma^W$ stands for iV for inner-V waves, RF for ring-fan waves, or oV for outer V-waves. (36a) yields $\beta \sim t/\sqrt{C}$ as $t \to 0$ with

$$C = \left\{ \begin{array}{l} 1+1/\sqrt{1+4\tau} \\ 1-1/\sqrt{1+4\tau} \\ 1+1/\sqrt{1-4\tau} \end{array} \right\} \text{ for } \left\{ \begin{array}{l} \text{inner-V} \\ \text{ring-fan} \\ \text{outer-V} \end{array} \right\} \text{ waves}$$

Thus, the integrand of (36d) is continuous at $t=0$.

The dispersion curve in the region $\alpha_i^- \le \alpha \le \alpha_i^+$ can be defined by the parametric representation

$$\left\{ \begin{array}{ll} k = f^2/(\sqrt{1/4+\tau\cos t}+1/2)^2 & \\ \alpha = k\cos t & \beta = k\sin t \end{array} \right\} \tag{37a}$$

with $-\pi \le t \le \pi$. In the limit $\tau \to 0$, the inner dispersion curve becomes a circle of radius $k=f^2$ centered at the origin of the Fourier plane. $\hat{\alpha}$ in (35) is given by

$$\hat{\alpha} = k\,[2\tau + (1-2F^2k)\,\cos t] \tag{37b}$$

(33a) and the relation $ds/\|\nabla D\| = -k\,dt/D_k$ yield

$$4\pi \left\{ \begin{array}{l} \phi_R^W \\ u_R^W \\ v_R^W \\ w_R^W \end{array} \right\} = \int_{-\pi}^{\pi} \frac{dt\ k}{\sqrt{1+4\tau\,\cos t}} \left\{ \begin{array}{l} i \\ \alpha \\ \beta \\ i\,k \end{array} \right\} \sum_{p=1}^{p=N} [\,\mathrm{erf}(\varphi_p) - 1\,]\, S_p^W \mathcal{E}_p^* \tag{37c}$$

The integrand of (37c) is continuous for $-\pi \le t \le \pi$ since ring waves exist only for $\tau < 1/4$. In the limit $F=0$, expressions (37) for the ring waves become

$$4\pi \left\{ \begin{array}{l} \phi_R^W \\ u_R^W \\ v_R^W \\ w_R^W \end{array} \right\} = f^2 \int_{-\pi}^{\pi} dt \left\{ \begin{array}{l} i \\ \alpha \\ \beta \\ i\,k \end{array} \right\} \sum_{p=1}^{p=N} [\,\mathrm{erf}(\varphi_p) - 1\,]\, S_p^W \mathcal{E}_p^* \tag{38}$$

with $(k, \alpha, \beta) = f^2\,(1, \cos t, \sin t)$ and $\varphi_p = [(\xi - x_p)\cos t + (\eta - y_p)\sin t]\, f^2/\sigma$. (38) defines time-harmonic waves associated with diffraction-radiation without forward speed.

Both the inner-V waves and the outer-V waves in (34a) contain real and imaginary parts. However, the waves given by the sum

$$\left\{ \begin{array}{l} \phi_V^W \\ \vec{u}_V^W \end{array} \right\} = \left\{ \begin{array}{l} \phi_{oV}^W + \phi_{iV}^W \\ \vec{u}_{oV}^W + \vec{u}_{iV}^W \end{array} \right\}$$

are real in the special case $f=0$, i.e. for steady ship waves. Specifically, (36) and the property that steady-flow spectrum functions satisfy the relation $S_p^W(-\alpha,-\beta) = \overline{S_p^W(\alpha,\beta)}$, with $\overline{Z}$ = complex conjugate of Z, show that steady ship waves can be expressed as

$$4\pi \begin{Bmatrix} \phi_V^W \\ u_V^W \\ v_V^W \\ w_V^W \end{Bmatrix} = \Re e \int_{-\infty}^{\infty} \frac{d\beta\ \alpha}{k-\nu} \begin{Bmatrix} i \\ \alpha \\ \beta \\ i\,k \end{Bmatrix} \sum_{p=1}^{p=N} [\,\mathrm{erf}(\varphi_p)+1\,]\, S_p^W \mathcal{E}_p^* \tag{39a}$$

$\Re e$ stands for the real part, the relation $ds/\|\nabla D\| = d\beta/D_\alpha = -k\,d\beta/\widehat{\alpha}$ was used, and

$$k = \nu + \sqrt{\nu^2+\beta^2} \qquad \alpha = \sqrt{k}/F \tag{39b}$$

with $\nu = 1/(2F^2)$. $\widehat{\alpha}$ in (35) is given by $\widehat{\alpha} = (1-2F^2k)\,\alpha$.

Rankine-Fourier decomposition : physical-space analysis

Consider the free-surface boundary condition (9). Define the coordinates (X,Y,Z) as

$$(\xi - x, \eta - y, \zeta + z) = \Lambda\,(X,Y,Z)$$

where Λ stands for a length scale. With respect to the Λ-scaled coordinates (X,Y,Z), the free-surface condition (9) becomes

$$G_Z - f^2\Lambda\,G + i\,2\tau\,G_X + (F^2/\Lambda)\,G_{XX} = 0 \tag{40}$$

In the particular case $F=0$, (40) becomes $G_Z - f^2\Lambda\,G = 0$. This condition yields

$$\begin{Bmatrix} G_Z \approx 0 \\ G \approx 0 \end{Bmatrix} \text{ if } \begin{Bmatrix} \Lambda \ll 1/f^2 \\ \Lambda \gg 1/f^2 \end{Bmatrix} \text{ i.e. for } \begin{Bmatrix} r' \ll 1/f^2 \\ r' \gg 1/f^2 \end{Bmatrix}$$

Thus, for time-harmonic flow without forward speed, the free surface acts like an infinitely rigid wall in the nearfield region $r' \ll 1/f^2$ and like an infinitely soft wall in the farfield region $r' \gg 1/f^2$. The alternative representations (12) therefore are complementary and appropriate in the nearfield and the farfield :

$$4\pi\,G = \begin{Bmatrix} -1/r - 1/r' + \mathcal{H} \\ -1/r + 1/r' + H \end{Bmatrix} \text{ for } \begin{Bmatrix} r' \ll 1/f^2 \\ r' \gg 1/f^2 \end{Bmatrix}$$

These nearfield and farfield approximations indicate that an "optimal" Rankine-Fourier decomposition of the Green function G related to the free-surface boundary condition (3c) is

$$4\pi\,G = -1/r - 1/r' + 2/r'' + \mathcal{F}^- \tag{41a}$$

where r' and r'' are defined by (1b) with $C^2 = 1/f^2$, and $\mathcal{F}^-$ is a Fourier component.

In the particular case $f=0$, (40) becomes $G_{XX} + (\Lambda/F^2)\, G_Z = 0$. This condition yields

$$\left\{ \begin{array}{c} G_{XX} \approx 0 \\ G_Z \approx 0 \end{array} \right\} \text{ if } \left\{ \begin{array}{c} \Lambda \ll F^2 \\ \Lambda \gg F^2 \end{array} \right\} \text{ i.e. for } \left\{ \begin{array}{c} r' \ll F^2 \\ r' \gg F^2 \end{array} \right\}$$

Thus, for steady flow, the free surface acts like an infinitely soft wall in the nearfield region $r' \ll F^2$ and like an infinitely rigid wall in the farfield region $r' \gg F^2$. The alternative representations (12) therefore are appropriate in the nearfield and the farfield :

$$4\pi G = \left\{ \begin{array}{c} -1/r + 1/r' + H \\ -1/r - 1/r' + \mathcal{H} \end{array} \right\} \text{ for } \left\{ \begin{array}{c} r' \ll F^2 \\ r' \gg F^2 \end{array} \right\}$$

These nearfield and farfield approximations indicate that an "optimal" Rankine-Fourier decomposition of the Green function G related to the free-surface condition (3b) is

$$4\pi G = -1/r + 1/r' - 2/r'' + \mathcal{F}^+ \tag{41b}$$

where r' and r'' are defined by (1b) with $C^2 = F^2$, and $\mathcal{F}^+$ is a Fourier component.

If $fF > 0$, the free-surface condition (40) yields

$$\left\{ \begin{array}{c} G_{XX} \approx 0 \\ G \approx 0 \end{array} \right\} \text{ if } \left\{ \begin{array}{c} \Lambda \to 0 \\ \Lambda \to \infty \end{array} \right\} \text{ i.e. for } \left\{ \begin{array}{c} r' \to 0 \\ r' \to \infty \end{array} \right\}$$

Thus, the free surface acts like an infinitely soft wall in both the nearfield $r' \to 0$ and the farfield $r' \to \infty$, and the Rankine-Fourier decomposition of the Green function

$$4\pi G = -1/r + 1/r' + H \tag{41c}$$

is "optimal" for the ship-motion free-surface condition (3a) with $fF > 0$.

Expressions (41) yield

$$4\pi G = -1/r + \left\{ \begin{array}{c} -1/r' + 2/r'' \\ 1/r' - 2/r'' \\ 1/r' \end{array} \right\} + \mathcal{F} \quad \text{if} \quad \left\{ \begin{array}{c} F=0 \\ f=0 \\ fF>0 \end{array} \right\} \tag{42a}$$

Here, r, r', r'' are defined by (1b) with C^2 given by

$$C^2 = \left\{ \begin{array}{c} 1/f^2 \\ F^2 \end{array} \right\} \text{ if } \left\{ \begin{array}{c} F=0 \\ f=0 \end{array} \right\} \tag{42b}$$

The Fourier-component $\mathcal{F}$ in (42a) is given in the next section.

Rankine-Fourier decomposition : Fourier-space analysis

The free-surface component G^F in expression (10a) for the Green function G corresponding to the free-surface boundary condition (9) is given by (11). Alternative forms of (11) are

$$4\pi G^F = \frac{1}{r'} + H^+ = \frac{-1}{r'} + H^- = \frac{1}{r'} - \frac{2}{r''} + \mathcal{F}^+ = \frac{-1}{r'} + \frac{2}{r''} + \mathcal{F}^- \tag{43}$$

The functions G^F, $H^\pm$, $\mathcal{F}^\pm$ are given by the right side of (13b) with k, $\mathcal{E}$, D_ε given by (2b) and (4), and

$$A = \left\{ \begin{array}{c} A^F \\ A^+ \\ A^- \\ \mathcal{A}^+ \\ \mathcal{A}^- \end{array} \right\} = \left\{ \begin{array}{c} [(f-F\alpha)^2/k+1]/2 \\ 1 \\ (f-F\alpha)^2/k \\ 1+[(f-F\alpha)^2/k-1]\,e^{-C^2 k} \\ (f-F\alpha)^2/k-[(f-F\alpha)^2/k-1]\,e^{-C^2 k} \end{array} \right\} \tag{44a}$$

as follows from (11), (2c) and (2d). The functions H^+ and H^- in (43) are identical to the previously-defined functions H and $\mathcal{H}$ (the notation $H^\pm$ is used here for convenience).

The theory of Fourier transforms, Lighthill (1970), shows that the farfield behaviors of the local components contained in the functions G^F, $H^\pm$, $\mathcal{F}^\pm$ are determined by the behaviors of the functions A^F/D, $A^\pm/D$, $\mathcal{A}^\pm/D$ at the origin $k=0$ of the Fourier plane. Conversely, the behaviors of these functions in the limit $k \to \infty$ determine the nearfield behaviors of the functions G^F, $H^\pm$, $\mathcal{F}^\pm$ in the physical space.

In the particular case $F=0$, we have $C^2=1/f^2$ and (44a) becomes

$$\left\{ \begin{array}{c} A^F \\ A^+ \\ A^- \\ \mathcal{A}^+ \\ \mathcal{A}^- \end{array} \right\} = \left\{ \begin{array}{c} (f^2/k+1)/2 \\ 1 \\ f^2/k \\ 1+(f^2/k-1)\,e^{-k/f^2} \\ f^2/k-(f^2/k-1)\,e^{-k/f^2} \end{array} \right\} \tag{44b}$$

The functions A^F, A^+ and $\mathcal{A}^+$ are finite in the limit $k \to \infty$, whereas the functions A^- and $\mathcal{A}^-$ are $O(f^2/k)$, i.e. vanish, in this limit. It follows that the functions H^- and $\mathcal{F}^-$ are less singular at the origin $r'=0$ than the functions G^F, H^+ and $\mathcal{F}^+$ in (43). In the limit $k \to 0$, the function A^- is $O(f^2/k)$, i.e. singular, whereas $\mathcal{A}^-$ is $O(1)$, i.e. finite. It follows that the local component contained

in the function $\mathcal{F}^-$ decays faster in the farfield $r' \to \infty$ than the local component associated with the function H^-. The decomposition (41a) is therefore preferable.

In the particular case $f = 0$, we have $C^2 = F^2$ and (44a) becomes

$$\begin{Bmatrix} A^F \\ A^+ \\ A^- \\ \mathcal{A}^+ \\ \mathcal{A}^- \end{Bmatrix} = \begin{Bmatrix} (F^2\alpha^2/k+1)/2 \\ 1 \\ F^2\alpha^2/k \\ 1+(F^2\alpha^2/k-1)\,e^{-F^2k} \\ F^2\alpha^2/k-(F^2\alpha^2/k-1)\,e^{-F^2k} \end{Bmatrix} \tag{44c}$$

In the limit $k \to \infty$, the functions A^F, A^- and $\mathcal{A}^-$ are $O(F^2\alpha^2/k)$, i.e. unbounded, whereas the functions A^+ and $\mathcal{A}^+$ are $O(1)$. The functions H^+ and $\mathcal{F}^+$ therefore are less singular at the origin $r' = 0$ than the functions G^F, H^- and $\mathcal{F}^-$ in (43). In the limit $k \to 0$, the function A^+ is finite but $\mathcal{A}^+$ is $O(F^2k)$ and thus vanishes. The local component contained in the function $\mathcal{F}^+$ therefore decays faster in the farfield $r' \to \infty$ than the local component corresponding to the function H^+, and the decomposition (41b) is preferable.

In the general case $fF > 0$, the functions A^F, A^- and $\mathcal{A}^-$ in (44a) are $O(F^2\alpha^2/k)$, i.e. unbounded, and the functions A^+ and $\mathcal{A}^+$ are $O(1)$ in the limit $k \to \infty$. In the limit $k \to 0$, the function A^+ is finite but the function $\mathcal{A}^+$ is $O(f^2/k)$, i.e. unbounded. Thus, the decomposition (41c) is preferable in this case.

The component $\mathcal{F}$ in expressions (42a) for the Green functions related to the free-surface conditions (3) is then defined by the Fourier superposition of elementary waves (13b), i.e.

$$\mathcal{F} = \lim_{\varepsilon \to +0} \frac{1}{\pi} \int_{-\infty}^{\infty} d\beta \int_{-\infty}^{\infty} d\alpha \; \frac{A}{D_\varepsilon} \; e^{k(\zeta+z)}\,\mathcal{E} \tag{45}$$

Here, k and $\mathcal{E}$ are given by (2b), the dispersion function D_ε is given by (4), and the amplitude function A is defined by (44) as

$$A = \begin{Bmatrix} f^2/k-(f^2/k-1)\,e^{-k/f^2} \\ 1+(F^2\alpha^2/k-1)\,e^{-F^2k} \\ 1 \end{Bmatrix} \text{ if } \begin{Bmatrix} F=0 \\ f=0 \\ fF>0 \end{Bmatrix} \tag{46}$$

Expressions (46) yield

$$A \sim \begin{Bmatrix} 2 \\ f^2/k \end{Bmatrix} \text{ as } k/f^2 \to \begin{Bmatrix} 0 \\ \infty \end{Bmatrix} \text{ if } F = 0$$

$$A \sim \left\{ \begin{matrix} F^2 k\,(1+\alpha^2/k^2\,) \\ 1 \end{matrix} \right\} \text{ as } F^2 k \to \left\{ \begin{matrix} 0 \\ \infty \end{matrix} \right\} \text{ if } f = 0$$

In the general case $fF>0$ and the special cases $f=0$ and $F=0$, (46) yield

$$\frac{A}{D} = \left\{ \begin{matrix} O(1) \\ O(1/k^2\,) \end{matrix} \right\} \text{ as } k \to \left\{ \begin{matrix} 0 \\ \infty \end{matrix} \right\}$$

and $A=1$ if $D=0$. Thus, the amplitude functions A defined by (46) are equal to 1 at a dispersion curve $D=0$, and the free-surface components defined by (46) and (13) yield identical farfield waves as one expects.

Expressions (42), (45) and (46) define the Green functions associated with the free-surface boundary conditions (3) in terms of elementary Rankine singularities and Fourier superpositions of elementary waves. The Rankine-singularity components in (42) account for the dominant terms in both the nearfield and farfield asymptotic approximations to the nonoscillatory local components included in the Green functions corresponding to (3). The foregoing method of extracting the leading nearfield and farfield local component from the Fourier component can in principle be pursued to obtain additional terms in the nearfield and farfield asymptotic approximations to the local components in free-surface Green functions.

Rankine and Fourier-Kochin representation of nearfield flows

The Rankine-Fourier decomposition process that has been expounded above for the simple case of free-surface Green functions is useful more widely, notably within the Fourier-Kochin approach. In fact, the potential and velocity representations, the Fourier-Kochin approach, and the Fourier-Rankine decomposition process yield remarkably simple analytical representations of nearfield flows for the three basic types of free-surface flows corresponding to (3), as is now explained.

Transformations of the wave-spectrum functions S^W, guided by the Rankine-Fourier decomposition process, can be performed for the purpose of obtaining practical representations of the local component ϕ^L, $\vec{u}^L$ in (32). These transformations express the wave-spectrum functions S^W given by (21) and (22) in terms of local-spectrum functions S^L and components that involve the dispersion function D and are dominant in both the limit $k \to \infty$ and the limit $k \to 0$:

$$S^W = D\,S^D + S^L \tag{47}$$

The dominant component $D\,S^D$ can be expressed in terms of distributions of Rankine singularities.

The potential ϕ and velocity $\vec{u}$ defined by the boundary-integral representations (14) and the Fourier-Kochin representations (32) of free-surface effects can then be expressed as

$$\begin{Bmatrix} \phi \\ \vec{u} \end{Bmatrix} = \begin{Bmatrix} \phi^W \\ \vec{u}^W \end{Bmatrix} + \begin{Bmatrix} \phi^R + \mu^\Sigma \phi_*^R - \mu^F \phi_F^R + \phi_\Gamma^R \\ \vec{u}^R + \mu^\Sigma \vec{u}_*^R - \mu^F \vec{u}_F^R + \vec{u}_\Gamma^R \end{Bmatrix} + \begin{Bmatrix} \phi_D^L + \phi_*^L \\ \vec{u}_D^L + \vec{u}_*^L \end{Bmatrix} \tag{48a}$$

with

$$\mu^\Sigma = \begin{Bmatrix} 1 \\ -1 \end{Bmatrix} \text{ if } \begin{Bmatrix} F=0 \\ F>0 \end{Bmatrix} \qquad \mu^F = \begin{Bmatrix} 1 \\ -1 \\ 0 \end{Bmatrix} \text{ if } \begin{Bmatrix} F=0 \\ f=0 \\ fF>0 \end{Bmatrix} \tag{48b}$$

The component ϕ^W, $\vec{u}^W$ on the right side of (48a) corresponds to the nearfield waves considered previously, and the other components represent a nonoscillatory local flow disturbance. Thus, the wave component ϕ^W, $\vec{u}^W$ is given by single Fourier integrals along the dispersion curves $D=0$. The Fourier integrals (33a) involve the wave-spectrum functions S^W defined by (21) and (22) in terms of distributions of elementary waves over the surface $\Sigma \cup \Gamma \cup \Sigma^F$.

The four components in the second group on the right side of (48a) are defined in terms of distributions of Rankine singularities. Specifically, the Rankine component ϕ^R, $\vec{u}^R$ is given by (15a) in terms of distributions of elementary Rankine singularities $R = -1/r$ over the boundary surface Σ. The Rankine component ϕ_*^R, $\vec{u}_*^R$ is also given by distributions of elementary Rankine singularities over the boundary surface Σ; specifically, the component ϕ_*^R, $\vec{u}_*^R$ is given by (15b) with R^* defined as

$$R^* = \begin{Bmatrix} -1/r' + 2/r'' \\ -1/r' \end{Bmatrix} \text{ if } \begin{Bmatrix} fF = 0 \\ fF > 0 \end{Bmatrix} \tag{49}$$

Here, r' and r'' are given by (1b) with C^2 defined by (42b). The function R^* is evidently related to the Rankine-Fourier decompositions (42) of the Green functions corresponding to the free-surface boundary conditions (3). The Rankine component ϕ_F^R, $\vec{u}_F^R$ in (48a) stems from the forcing term p in (3) and is given by

$$4\pi \begin{Bmatrix} \phi_F^R \\ u_F^R \\ v_F^R \\ w_F^R \end{Bmatrix} = 2 \int_{\Sigma^F} d\mathcal{A}\, p \begin{Bmatrix} (1/r)'' \\ (1/r)''_\xi \\ (1/r)''_\eta \\ (1/r)''_\zeta \end{Bmatrix}$$

The Rankine component ϕ_Γ^R, $\vec{u}_\Gamma^R$ in (48a) is given by distributions of Rankine singularities over the boundary curve Γ.

Finally, the two components in the third group on the right side of (48a) are Fourier components that are defined by single Fourier integrals along the dispersion curves and double Fourier integrals, as given by (30) and (29b)-(29c). These Fourier integrals are defined in terms of the local-spectrum function S^L in (47). The integrands of the double Fourier integrals defining the component ϕ_*^L, $\vec{u}_*^L$ are finite at $k=0$ and continuous everywhere in the Fourier plane, and decay rapidly as $k \to \infty$.

The Rankine component ϕ_Γ^R, $\vec{u}_\Gamma^R$ and the Fourier components ϕ_D^L, $\vec{u}_D^L$ and ϕ_*^L, $\vec{u}_*^L$ in the nearfield flow representation (48), called Rankine and Fourier-Kochin representation, will be given elsewhere. The Rankine and Fourier-Kochin representation of nearfield flows does not involve the special functions that appear in the integral-representations of the Green functions associated with the free-surface boundary conditions for steady and time-harmonic ship waves given in Noblesse (1981) and Chen (1999). In fact, the Rankine and Fourier-Kochin representation (48a) is entirely defined in terms of the elementary solutions (1), and thus is remarkably simple.

Iterative solution procedures and related approximations

Numerical calculations of free-surface potential flows due to ships and offshore structures have traditionally relied on the computation of influence coefficients associated with a discretization of an integral equation obtained from the classical potential representation. An alternative approach based on an iterative solution procedure can be advantageous, and can provide useful analytical approximations. An example is the slender-ship approximation given in Noblesse (1983) and Noblesse and Triantafyllou (1983). This approximation defines the steady velocity field $\vec{u}(\vec{\xi})$ due to a ship explicitly in terms of the speed and shape of the ship :

$$\vec{u}(\vec{\xi}) = \int_\Sigma d\mathcal{A}(\vec{x})\, n^x(\vec{x})\, \nabla_\xi G(\vec{\xi},\vec{x}) + F^2 \int_\Gamma d\mathcal{L}(\vec{x})\, [\, n^x(\vec{x})\,]^2\, t^y(\vec{x})\, \nabla_\xi G(\vec{\xi},\vec{x}) \tag{50}$$

The slender-ship approximation (50) is a generalization of the Michell thin-ship approximation. Specifically, the Michell approximation differs from (50) in that it defines $\vec{u}$ in terms of a distribution of sources, with strength $2\,n^x$, over the ship centerplane $y=0$ instead of a distribution of sources of strength n^x over the port and starboard sides of the actual ship surface Σ. In addition, there is no distribution of sources around the waterline Γ in Michell's approximation.

The wave component $\vec{u}^W$ in the decomposition $\vec{u} = \vec{u}^W + \vec{u}^L$ is given by the Fourier-Kochin representation (33), which can be expressed as in Yang et al. (2000b). The wave-spectrum function

S^W corresponding to the slender-ship approximation (50) is defined by

$$S^W = \int_\Sigma d\mathcal{A}\; n^x\, e^{k\,z}\, \mathcal{E}_0 + F^2 \int_\Gamma d\mathcal{L}\; (n^x)^2\, t^y\, \mathcal{E}_0$$

with $\mathcal{E}_0 = e^{i(\alpha x + \beta y)}$. The local component $\vec{u}^L$ can be effectively evaluated from (50) with the Green function G taken as the simple analytical approximation to the local component G^L defined by (42) as

$$4\pi G^L \approx -1/r + 1/r' - 2/r''$$

Here, r, r', r'' are defined by (1b) with $C^2 = F^2$.

At the ship hull surface Σ, the velocity field $\vec{u}$ given by the slender-ship approximation (50) can be modified using the transformation

$$\vec{u}_* = \vec{u} - (\vec{u}\cdot\vec{n} - n^x)\,\vec{n} \tag{51}$$

This transformation yields $\vec{u}_*\cdot\vec{n} = n^x$ and thus ensures that the velocity distribution $\vec{u}_*$ at the hull surface satisfies the hull boundary condition. The hull-condition transformation (51) can be applied to any velocity distribution $\vec{u}$ computed at a ship hull surface. In particular, (51) shows that the velocity distribution $\vec{u}_*$ associated with the trivial velocity distribution $\vec{u} = 0$ is given by $\vec{u}_* = n^x\,\vec{n}$. This velocity distribution is normal to the ship surface Σ and evidently satisfies the hull boundary condition $\vec{u}_*\cdot\vec{n} = n^x$. The velocity distribution $\vec{u}_* = n^x\,\vec{n}$ in fact corresponds to the slender-ship approximation (50). The practical usefulness, notably for hull-form optimization, of this remarkably simple approximation is demonstrated in Letcher et al. (1987), Wyatt and Chang (1994), and Yang et al. (2000b).

Conclusion

Four fundamental analytical representations have been given for time-harmonic ship waves, steady ship waves, and wave diffraction-radiation without forward speed :

1. The potential and velocity representations (14)-(18) define a flow within a free-surface potential-flow region in terms of the flow at a boundary surface : the potential representation defines the velocity potential ϕ in terms of boundary values of ϕ and its normal derivative $\partial\phi/\partial n$, and the velocity representation obtained in Noblesse (2000) defines the velocity $\vec{u}$ in terms of boundary values of $\vec{u}$. These boundary-integral representations, given here for deep water, can be extended to uniform finite water depth. The velocity representation defines $\vec{u}$ within a flow domain in terms

of source and vortex distributions with strength equal to the normal and tangential components of $\vec{u}$ at the boundary surface. Thus, the velocity representation does not involve the potential ϕ, and can be used to couple a nearfield flow calculation method based on the Euler or RANS equations (for which a velocity potential cannot be defined) and a farfield potential flow representation. The velocity representation defines $\vec{u}$ in terms of first derivatives of the Green function G (whereas $\vec{u}$ can only be obtained from the potential representation via analytical differentiation of ϕ, which involves second-order derivatives of G, or via numerical differentiation of ϕ).

2. A practical representation of the super Green function $\mathcal{G}$ defined by (23) has been given. The dispersion functions D, D' and the amplitude function A in (23) are generic. Thus, the super Green function (23) is representative of a broad class of dispersive waves (including water waves in finite uniform water depth and internal waves in a density-stratified fluid) generated by an arbitrary distribution of singularities (e.g. source, dipole, vortex sheets). Expression (31) provides a formal decomposition of the singular double Fourier integral (23) in terms of a wave component and a local component. The wave component $\mathcal{G}^W$ in this decomposition is defined by (26) in terms of single Fourier integrals along the dispersion curves associated with the dispersion relation $D=0$. The local component $\mathcal{G}^L$ is given by (29) and (30). The single Fourier integrals (26a) and (30a) and the double Fourier integral (29b) can be evaluated in a straightforward and very efficient manner if the amplitude function A is not rapidly oscillatory (as is the case in practice if the boundary surface is divided into patches). The single Fourier integrals (26a) and (30a) can obviously be combined.

3. The Fourier-Kochin approach and the Fourier representation of super Green functions have been used to express the potential ϕ and velocity $\vec{u}$ defined by the boundary-integral representations (14)-(18) as the sum of a wave component ϕ^W, $\vec{u}^W$ and a local component that represents a nonoscillatory local flow disturbance. The wave component is given by the single Fourier integrals (33), where summation is performed over all the patches that represent the surface $\Sigma \cup \Gamma \cup \Sigma^F$, and the wave-spectrum function S_p^W is defined by (21) and (22) in terms of distributions of elementary waves over patch p. Thus, the farfield and nearfield waves generated by a velocity distribution at a boundary surface are defined in terms of remarkably simple Fourier superpositions of elementary waves over the boundary surface. Specifically, time-harmonic ship waves are defined by (34) with (36) and (37); time-harmonic waves in the special case $F=0$ (no forward speed) and steady ship waves (zero-frequency limit $f=0$) are respectively given by (38) and (39). The Fourier-Kochin wave representation has been obtained from the potential representation in Noblesse and Yang

(1995) and from the velocity representation in Noblesse (2000).

4. The Fourier-Kochin approach, the Fourier representation of super Green functions, and the Rankine-Fourier decomposition process, expounded here for free-surface Green functions, show that the potential ϕ and velocity $\vec{u}$ defined by the boundary-integral representations (14)-(18) can be expressed as in (48). The nearfield flow representation (48) extends the Fourier-Kochin representation of waves given by (33) and (21)-(22). Indeed, the wave component ϕ^W, $\vec{u}^W$ in (48a) corresponds to the nearfield waves given by the Fourier-Kochin wave representation. The other components in (48a) represent local flow disturbances. These local-flow components consist of Rankine components and Fourier components that are respectively given by distributions of elementary Rankine singularities and elementary waves over the boundary surface Σ, the boundary curve Γ, and (eventually) the mean free-surface plane Σ^F (if $p \neq 0$). The Fourier components are given by single Fourier integrals along the dispersion curves and double Fourier integrals, as in (30) and (29b)-(29c). The integrands of the double Fourier integrals defining ϕ_*^L, $\vec{u}_*^L$ are finite at $k=0$ and continuous everywhere in the Fourier plane, and decay rapidly as $k \to \infty$. The Rankine and Fourier-Kochin representation (48) of nearfield flows only involves elementary functions and is remarkably simple.

The foregoing four analytical representations, which are the major results underlying the Fourier-Kochin theory, provide a new mathematical basis for computing free-surface flows about nonlifting and lifting bodies using free-surface Green functions. Practical applications of the Fourier-Kochin representation of waves are given (for the case of steady ship waves) in Guillerm and Alessandrini (1999) and Yang et al. (2000a,b). Specifically, the Fourier-Kochin representation of steady ship waves is coupled with nearfield calculations based on the RANS and the Euler equations in Guillerm and Alessandrini (1999) and Yang et al. (2000a), respectively, and is applied to the design of a wave cancellation multihull ship in Yang et al. (2000b). The representation of super Green functions has also been used in Noblesse and Chen (1995) to obtain a simple representation of the Green function for wave diffraction-radiation at low forward speed in terms of the Green function for wave diffraction-radiation without forward speed. The Fourier-Kochin theory is currently being applied to time-harmonic ship waves.

Yang et al. (2000a,b) show that calculations based on the Fourier-Kochin approach are remarkably efficient. This efficiency stems from the fact that evaluation of the wave component ϕ^W, $\vec{u}^W$ and the local components ϕ_D^L, $\vec{u}_D^L$ and ϕ_*^L, $\vec{u}_*^L$ in the Rankine and Fourier-Kochin nearfield flow

representation (48a) involves two $O(N)$ operations : (i) evaluation of the wave and local spectrum functions S^W and S^L, which is a $O(N^{\text{panels}})$ operation where N^{panels} stands for the number of panels used to approximate the boundary surface, and (ii) evaluation of the Fourier integrals (26a), (30a) and (29b), a $O(N^{\text{points}})$ operation where N^{points} is the number of points at which the flow is computed. Thus, evaluation of the free-surface components in the Rankine and Fourier-Kochin representation involves $O(N^{\text{panels}})+O(N^{\text{points}})$ operations, instead of $O(N^{\text{panels}}) \times O(N^{\text{points}})$ operations for the classical Green function method. This property directly follows from the identity

$$e^{k(\zeta+z)-i[\alpha(\xi-x)+\beta(\eta-y)]} = e^{k\zeta-i(\alpha\xi+\beta\eta)}\, e^{kz+i(\alpha x+\beta y)}$$

which is used in the Fourier-Kochin representation of free-surface effects, but is ignored in the classical Green function approach. Evaluation of the Rankine components ϕ^R, $\vec{u}^R$ and ϕ^R_*, $\vec{u}^R_*$ in (26a) is a $O(N^{\text{panels}}) \times O(N^{\text{points}})$ operation, which indeed consumes the largest share of computing time for the relatively large values of N^{panels} and N^{points} that are required at low speed and/or high wave frequencies (N is approximately proportional to $1/F^2$ and f^2).

Although the free-surface boundary conditions (3) correspond to Kelvin linearization about the uniform stream opposing the ship speed, the nonhomogeneous forcing term p in (3) can account for linearization about a more complex base flow, e.g. flow about a ship in the presence of a rigid free surface. Thus, the potential and velocity representations, the Fourier-Kochin wave representation, and the Rankine and Fourier-Kochin nearfield flow representation, can be used within the context of various free-surface linearizations.

References

Abramowitz, M. and Stegun, I.A. (1965) *Handbook of Mathematical Functions*, Dover

Chen, X.B. (1999) *An introductory treatise on ship-motion Green functions*, 7th Intl Conf. Numerical Ship Hydrodynamics, Nantes, pp. 1.1.1-21

Guillerm, P.E. and Alessandrini B. (1999) *3D RANSE-potential coupling using a Fourier-Kochin approach*, 7th Intl Conf. Numerical Ship Hydrodynamics, Nantes, pp. 2.6.1-11

Letcher, J.S. Jr., Marshall, J.K., Oliver, J.C. III and Salvesen, N. (1987) *Stars & Stripes*, Scientific American, 257: 34-40

Lighthill, M.J. (1970) *Introduction to Fourier analysis and generalized functions*, Cambridge University Press, 79 pp.

Noblesse, F. (1981) *Alternative integral representations for the Green function of the theory of ship wave resistance*, Jl Engineering Mathematics 15:241-265

Noblesse, F. (1982) *The Green function in the theory of radiation and diffraction of regular water waves by a body*, Jl Engineering Mathematics 16:137-169

Noblesse, F. (1983) *A slender-ship theory of wave resistance*, Jl Ship Research 27:13-33

Noblesse, F. (2000) *Velocity Representation of Free-Surface Flows and Fourier-Kochin Representation of Waves*, NSWCCD-TR-2000/012

Noblesse, F. and Chen, X.B. (1995) *Decomposition of free-surface effects into wave and near-field components*, Ship Technology Research 42:167-185

Noblesse, F. and Chen, X.B. (1997) *Far-field and near-field dispersive waves*, Ship Technology Research 44:37-43

Noblesse, F., Chen, X.B. and Yang, C. (1999) *Generic super Green functions*, Ship Technology Research 46:81-92

Noblesse, F. and Triantafyllou, G. (1983) *Explicit approximations for calculating potential flow about a body*, Jl Ship Research 27:1-12

Noblesse, F. and Yang, C. (1995) *Fourier-Kochin formulation of wave diffraction-radiation by ships or offshore structures*, Ship Technology Research 42:115-139

Noblesse, F. and Yang, C. (1996) *Fourier representation of near-field free-surface flows*, Ship Technology Research 43:19-37

Ponizy, B., Noblesse, F., Ba, M., Guilbaud, M. (1994) *Numerical evaluation of free-surface Green functions*, Jl Ship Research 38:193-202

Wyatt, D.C. and Chang, P.A. (1994) *Development and assessment of a total resistance optimized bow for the AE 36*, Marine Technology 31: 149-160

Yang, C., Löhner, R. and Noblesse, F. (2000a) *Farfield extension of nearfield steady ship waves*, Ship Technology Research 47:22-34

Yang, C., Noblesse, F., Löhner R. and Hendrix, D. (2000b) *Practical CFD applications to design of a wave cancellation multihull ship*, 23rd Symp. on Naval Hydrodynamics, Val de Reuil, France

Figures

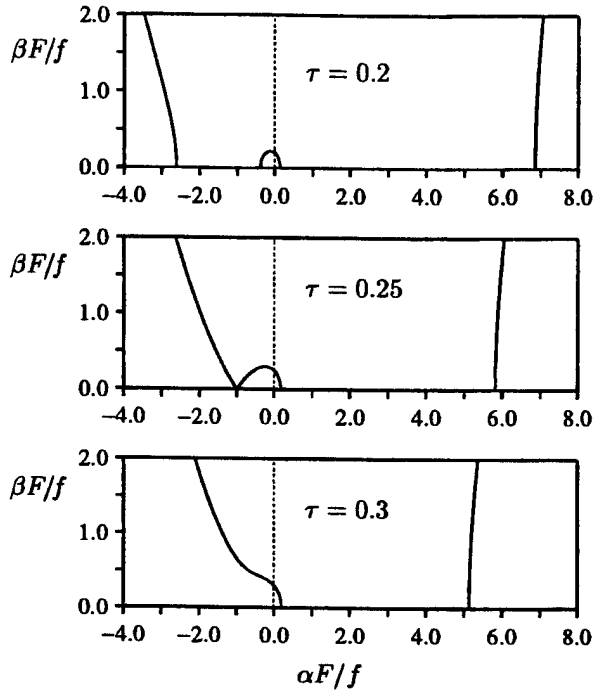

Fig.1 Dispersion curves for $\tau = 0.2, 0.25$ and 0.3 in the Fourier plane $(\alpha, \beta)F/f$

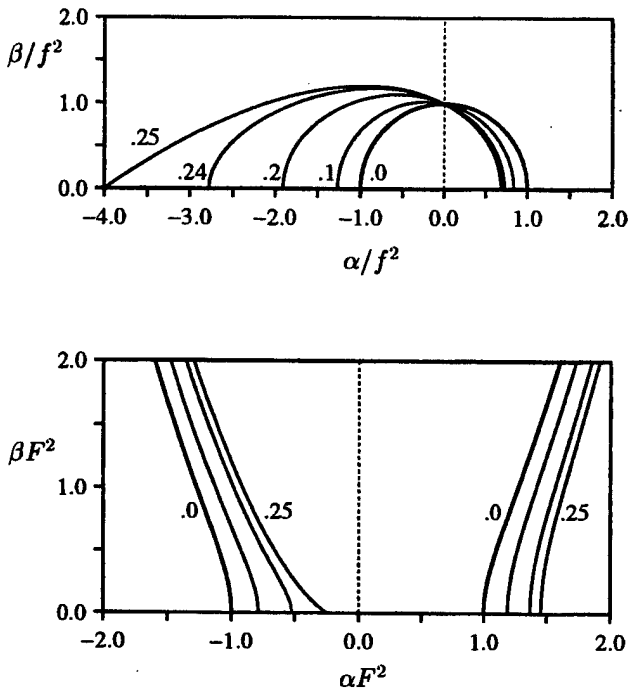

Fig.2 Dispersion curves in the Fourier planes $(\alpha, \beta)/f^2$ and $(\alpha, \beta)F^2$

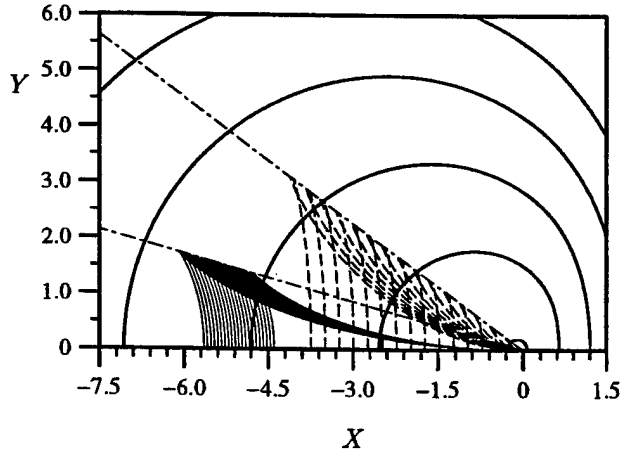

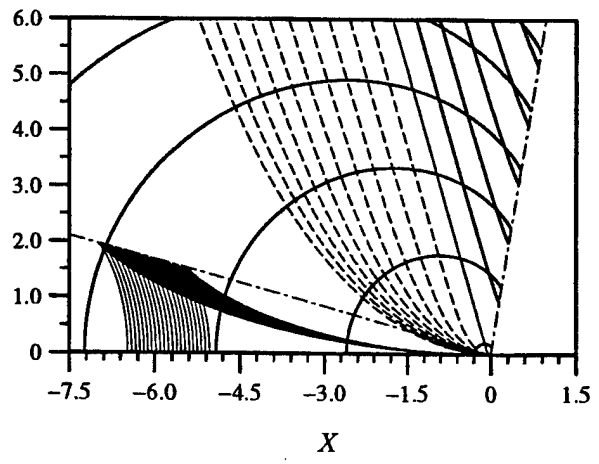

Fig.3 Constant-phase curves for $\tau = 0.24$ (left) and $\tau = 0.26$ (right).

Appendix 1

An elementary verification of (2a) is given here. Expression (2a) yields

$$\frac{1}{r} = \frac{1}{2\pi}\int_{-\infty}^{\infty} d\beta \int_{-\infty}^{\infty} d\alpha \, \frac{1}{k} \left\{ \begin{matrix} e^{-k(\zeta - z)} \\ e^{k(\zeta - z)} \end{matrix} \right\} \mathcal{E} \quad \text{if} \left\{ \begin{matrix} \zeta > z \\ \zeta < z \end{matrix} \right\}$$

It follows that $\nabla_\xi^2 (1/r) = 0$ if $\zeta \neq z$. The flux through the two planes $\zeta = z \pm 0$ is given by

$$[\partial(-1/r)/\partial\zeta]_{z-0}^{z+0} = \frac{1}{\pi}\int_{-\infty}^{\infty} d\alpha \; e^{-i\alpha(\xi - x)} \int_{-\infty}^{\infty} d\beta \; e^{-i\beta(\eta - y)} = 4\pi \, \delta(\xi - x)\, \delta(\eta - y)$$

Thus, (2a) represents the velocity potential created at $\vec{\xi}$ by a unit source located at $\vec{x}$.

Appendix 2

Expressions (11a) and (2b) show that that the free-surface component G^F in (10a) satisfies the Laplace equation. Expressions (10), (2a) with $\zeta > z$, and (11a) yield

$$4\pi G = \lim_{\varepsilon \to +0} \frac{1}{2\pi}\int_{-\infty}^{\infty} d\beta \int_{-\infty}^{\infty} d\alpha \, (\, 2A^F e^{k\zeta} - \frac{D_\varepsilon}{k} e^{-k\zeta}\,) \frac{e^{kz}\mathcal{E}}{D_\varepsilon}$$

At the free-surface plane $\zeta = 0$ we then have

$$G_\zeta - f^2 G + i\,2\tau\, G_\xi + F^2 G_{\xi\xi} - \varepsilon\,(\,ifG + FG_\xi\,) =$$
$$\lim_{\varepsilon \to +0} \frac{1}{8\pi^2}\int_{-\infty}^{\infty} d\beta \int_{-\infty}^{\infty} d\alpha \, \frac{\Lambda}{D_\varepsilon} e^{kz}\mathcal{E} \qquad \text{with}$$

$$\Lambda = 2k\,A^F + D_\varepsilon - (f - F\alpha)\,(f - F\alpha + i\varepsilon\,)(\,2A^F - D_\varepsilon/k\,)$$

Expressions (4) and (11b) yield $\Lambda \sim i\varepsilon\, DD'/k$ as $\varepsilon \to 0$. Thus, $\Lambda = O(\varepsilon)$ if $D \neq 0$ and $\Lambda = O(\varepsilon^2)$ if $D = 0$ as $\varepsilon \to 0$.

Appendix 3

The representation (28) holds if

$$\mathcal{G}_2^W = \int_{-\infty}^{\infty} d\beta \int_{-\infty}^{\infty} d\alpha \sum_{D=0} E_j\, A_j \frac{\mathcal{E}}{D} = \sum_{D=0} \int_{D=0} ds \int_{-\infty}^{\infty} dn \, E_j\, A_j \frac{\mathcal{E}}{D}$$

Here, $\mathcal{E} = e^{-i(X\alpha + Y\beta)}$, and ds and dn are the differential elements of length along a dispersion curve $D = 0$ and its normal ∇D. The relation $dn = dD/\|\nabla D\|$ and expression (28b) show that the foregoing expression is identical to (12) in Noblesse et al. (1999).

DISTRIBUTION LIST

	Copies
DOD CONUS	
ATTN CODE33 (S LEKOUDIS)	1
ATTN CODE 333 (P PURTELL)	1
ATTN CODE 333 (E ROOD)	1
OFFICE OF NAVAL RESEARCH	
BALLSTON CENTRE TOWER ONE	
800 NORTH QUINCY ST	
ARLINGTON VA 22217-5660	
NON DOD	
ATTN PROF R LOHNER	1
ATTN DR C YANG	1
GEORGE MASON UNIV MS 4 C7	
COMPUTATIONAL SCIENCES &	
INFORMATICS	
FAIRFAX VA 22030	
ATTN PROF R F BECK	1
UNIVERSITY OF MICHIGAN NA+ME	
2600 DRAPER ROAD	
ANN ARBOR MI 48109-2145	
ATTN PROF W W SCHULTZ	1
UNIVERSITY OF MICHIGAN ME+AM	
313 AUTO LAB	
ANN ARBOR MI 48109-2121	
ATTN PROF P D SCLAVOUNOS (5-326C)	1
ATTN PROF J N NEWMAN (5-324)	1
MASSACHUSETTS INST OF TECHNOLOGY	
77 MASSACHUSETTS AVE	
CAMBRIDGE MA 02139	
ATTN PROF W C WEBSTER	1
UNIVERSITY OF CALIFORNIA	
MCLAUGHLIN HALL (ROOM 308)	
BERKELEY CA 94720-1702	
ATTN PROF J V WEHAUSEN	1
ATTN PROF R W YEUNG	1
UNIVERSITY OF CALIFORNIA	
NAVAL ARCHITECTURE & OFFSHORE ENGG	
BERKELEY CA 94720-1780	
ATTN PROF M P TULIN	1
UNIV OF CALIFORNIA AT SANTA BARBARA	
OCEAN ENGG LAB	
6740 CORTONA DRIVE	
GOLETA CA 93117	

	Copies
ATTN PROF S GRILLI	1
UNIV OF RHODE ISLAND	
DEPT OF OCEAN ENG	
211 SHEETS BUILDING	
NARRAGANSETT RI 02882	
ATTN DR T T HUANG	1
NEWPORT NEWS SHIPBUILDING	
AIRPORT PLAZA 1 SUITE 1100	
2711 SOUTH JEFFERSON DAVIS HIGHWAY	
ARLINGTON VA 22202-4028	
ATTN DR W M LIN	1
SAIC	
134 HOLIDAY COURT SUITE 318	
ANNAPOLIS MD 21401	
ATTN PROF R EATOCK TAYLOR	1
UNIVERSITY OF OXFORD	
DEPT OF ENGINEEERING SCIENCE	
PARKS ROAD	
OXFORD OX1 3PJ	
UNITED KINGDOM	
ATTN PROF D V EVANS	1
UNIVERSITY OF BRISTOL	
SCHOOL OF MATHEMATICS	
UNIVERSITY WALK	
BRISTOL BSS 1TW	
UNITED KINGDOM	
ATTN DR F URSELL	1
28 OLD BROADWAY	
MANCHESTER M20 3DF	
UNITED KINGDOM	
ATTN PROF H SOEDING	1
ATTN DR V BERTRAM	1
INSTITUTE FUR SCHIFFBAU	
LAMMERSIETH 90	
HAMBURG D-22305	
GERMANY	
ATTN PROF S D SHARMA	1
MERCATOR UNIV	
INSTITUTE OF SHIP TECHNOLOGY	
BUILDING BK	
DUISBURG D-47048	
GERMANY	

	Copies
ATTN PROF O FALTINSEN NORWEGIAN UNIV OF SCIENCE AND TECHNOLOGY DIVISION OF MARINE HYDRODYNAMICS TRONDHEIM N-7034 NORWAY	1
ATTN PROF E PALM	1
ATTN PROF J GRUE UNIVERSITY OF OSLO DEPT OF MATHEMATICS P O B 1053 BLINDERN OSLO N-0316 NORWAY	1
ATTN PROF A J HERMANS DELFT UNIV OF TECHNOLOGY DEPT OF APPLIED MATHEMATICS P O B 5031 DELFT 2600 GA THE NETHERLANDS	1
ATTN DR R HUIJSMANS	1
ATTN DR H RAVEN MARIN P O B 28 WAGENINGEN 6700 AA THE NETHERLANDS	1
ATTN DR X B CHEN	1
ATTN DR S MALENICA BUREAU VERITAS 17BIS PLACE DES REFLETS LA DEFENSE 2 COURBEVOIE 92400 FRANCE	1
ATTN PROF B MOLIN	1
ATTN PROF Y M SCOLAN ESIM DEPT GENIE MER TECHNOPOLE DE CHATEAU-GOMBERT MARSEILLE 13451 CEDEX 20 FRANCE	1
ATTN PROF B ALESSANDRINI	1
ATTN PROF A CLEMENT	1
ATTN PROF G DELHOMMEAU	1
ATTN PROF P FERRANT	1
ATTN P E GUILLERM ECN-LMF DIV HYDRODYNAMIQUE NAVALE 1 RUE DE LA NOE B P 92101 NANTES 44300 CEDEX 3 FRANCE	1

	Copies
ATTN PROF M GUILBAUD	1
ATTN PROF M BA CEAT 43 AVE DE L'AERODROME POITIERS 86036 FRANCE	1
ATTN DR M LANDRINI INSEAN ITALIAN SHIP MODEL BASIN VIA DI VALLERANO 139 ROMA 00128 ITALY	1
ATTN DR J P BRESLIN CALLE DINAMARCA 7 SAN MIGUEL DE SALINAS ALICANTE 03193 SPAIN	1
ATTN PROF T MILOH TEL AVIV UNIV DEPT OF FLUID MECHANICS AND HEAT TRANSFER RAMAT AVIV 69978 ISRAEL	1
ATTN PROF K NAKATAKE KYUSHU UNIVERSITY DEPARTMENT OF NAVAL ARCHITECTURE 6-10-1 HAKOZAKI, HIGASHI-KU FUKUOKA 812-81 JAPAN	1
ATTN PROF M OHKUSU	1
ATTN PROF M KASHIWAGI KYUSHU UNIV RESEARCH INST FOR APPL MECHANICS 6-1 KASUGA-KOEN KASUGA-CITY FUKUOKA 816-8580 JAPAN	1
ATTN PROF H IWASHITA HIROSHIMA UNIV DEPT OF ENGINEERING SYSTEMS 1-3-1 KAGAMIYAMA HIGASHI-HIROSHIMA 739 JAPAN	1
ATTN PROF K MORI HIROSHIMA UNIV 1-4-1 KAGAMIYAMA HIGASHI-HIROSHIMA 724 JAPAN	1

		Copies
ATTN PROF L DOCTORS UNIVERSITY OF NEW SOUTH WALES SCHOOL OF MECH ENG SYDNEY NSW 2052 AUSTRALIA		1
ATTN PROF E O TUCK UNIV OF ADELAIDE APPLIED MATH DEPT GPO BOX 498 ADELAIDE SA 500 AUSTRALIA		1
ATTN PROF J A P ARANHA UNIV DE SAO PAULO DEPT OF NAVAL AND OCEAN ENG CX POSTAL 61548 – CEP 05424-970 SAO PAULO SP BRASIL		1
INTERNAL DISTRIBUTION		
011	J CORRADO	1
0112	J BARKYOUMB	1
0112	F HALSALL	1
0114	K H KIM	1
26	G EVERSTINE	1
3442	TIC(C)	1
5000	W B MORGAN	1
5040	W C LIN	1
5050	B WEBSTER	1
5050	A REED	1
5060		9
5080	H LIU	1
5100	W DAY	1
5200	P CHANG	1
5200	D CUSANELLI	1
5200	S FISHER,	1
5200	T FU	1
5200	D HENDRIX	1
5200	B HILL	1
5200	R HURWITZ	1
5200	G KARAFIATH	1
5200	C W LIN	1
5200	J LEE	1
5200	W LIU	1
5200	I MUTNICK	1
5200	L O'CONNELL,	1
5200	A S PERCIVAL	1
5200	T RATCLIFFE	1
5200	R STENSON	1
5200	W WILSON	1
5300	D COAKLEY	1
5300	R IMBER	1
5400	R COLEMAN	1
5400	C DAI,	1
5400	D FRY,	1
5400	J GORSKI,	1
5400	S GOWING,	1
5400	H HAUSSLING	1
5400	S JESSUP,	1
5400	Y T LEE	1
5400	L MULVIHILL	1
5400	Y T SHEN	1
5400	J TELSTE	1
5400	M B WILSON	1
5400	C I YANG	1
5500	M DAVIS,	1
5500	R Q LIN,	1
5500	W MCCREIGHT	1
5500	L MOTTER	1
5500	J O'DEA	1
5500	F NOBLESSE	50
5600	M S CHANG	1
5600	R CURPHEY	1
5600	W FALLER,	1
5600	J FELDMAN,	1
5600	Y HONG	1
5600	Y H KIM	1
5600	I Y KOH	1
5600	T MORAN	1
5600	C H SUNG	1
702	M STRASBERG	1
703	G MAIDANIC	1
705	D FEIT	1